10.1071/CH19271_AC

Australian Journal of Chemistry 2019, 72(10), 848-851

Supplementary Material

Polyacids as Modulators for the Synthesis of UiO-66

Kyle C. Bentz,[A] Sergio Ayala Jr,[A] Mark Kalaj,[A] and Seth M. Cohen[A,B]

[A]Department of Chemistry and Biochemistry, University of California, San Diego, La Jolla, CA 92093, USA.
[B]Corresponding author. Email: scohen@ucsd.edu

SYNTHESIS AND CHARACTERIZATION

Synthetic procedures

General. All reagents and solvents were purchased from commercially available sources and used as received, unless otherwise noted. Acrylic acid was passed through a column of basic alumina prior to use.

Synthesis of UiO-66. To a 20 mL scintillation vial was added terephthalic acid (10 mg, 0.060 mmol), zirconium chloride (14 mg, 0.060 mmol), dimethylformamide (DMF) (3.5 mL), and acid modulator. Example quantities of acid modulator, 1 equivalent: acrylic acid (AA) (3.4 μL, 0.060 mmol); poly(acrylic acid) PAA (4.8 mg, 0.060 mmol); benzoic acid (BA) (7.3 mg, 0.060 mmol); poly(vinylbenzoic acid) (PBA) (10 mg, 0.060 mmol). The vial was sealed with a Teflon-lined cap, placed in a preheated oven at 120 °C for 24 hours, and washed by centrifugation and redispersion in DMF two times, CH_2Cl_2 two times, and MeOH . Particles were dried *in vacuo* overnight prior to analysis.

Reversible addition-fragmentation chain transfer polymerization of acrylic acid. To a 10 mL Schlenk flask were added acrylic acid (1.00 g, 13.9 mmol), azobisisobutyronitrile (7.6 mg, 0.046 mmol), 2-(dodecylthiocarbonothioylthio)-2-methylpropionic acid (101 mg, 0.28 mmol), and tetrahydrofuran (6.9 mL). The solution was purged with Ar for 15 minutes, then placed in an oil bath at 60 °C for 16 hours. The polymerization was quenched by exposed the flask to air and bringing to room temperature. The polymer was recovered by precipitating into diethyl ether and drying *in vacuo* (0.652 g, 59%). ^{1}H NMR (500 MHz, d_6-DMSO): δ 12.22 (s, 55H), 2.33-2.10 (b, 51H), 1.66-1.37 (b, 84H), 0.86 (t, 3H). $M_{n,\,NMR}$ = 3,960 g/mol, $M_{n,\,GPC\ (PEG\ standards)}$ = 12,200 g/mol, Đ = 1.04.

Synthesis of vinylmethylbenzoate. To a 250 mL round bottom flask was added methyltriphenyl phosphonium bromide (2.54 g, 7.10 mmol) and dry tetrahydrofuran (60 mL). The flask was cooled to 0 °C, followed by the dropwise addition of *n*-BuLi (4.3 mL, 1.6 M in hexanes). The mixture

was stirred for 15 minutes then a solution of formylmethylbenzoate (1.00 g, 6.1 mmol, in 5 mL THF) was added slowly and stirred for an additional 15 minutes at 0 °C. The reaction mixture was then allowed to warm to room temperature and stirred for an additional 2 hours before being quenched with water (20 mL). The product was extracted with CH_2Cl_2 (3×50 mL) and purified by silica chromatography eluting in 100:0 to 80:20 hexane:ethyl acetate to give a white solid (0.832 mg, 81%). ^{1}H NMR (500 MHz, d_6-DMSO): δ 8.00 (d, 2H), 7.47 (d, 2H), 6.76 (m, 1H), 5.84 (d, 1H), 5.37 (d, 1H), 3.91 (s, 3H).

Reversible addition-fragmentation chain transfer polymerization of vinylmethylbenzoate. To a 10 mL Schlenk flask were added vinylmethylbenzoate (0.50 g, 3.1 mmol), azobisisobutyronitrile (1.6 mg, 0.0098 mmol), 2-(dodecylthiocarbonothioylthio)-2-methylpropionic acid (22 mg, 0.061 mmol), and 1,4-dioxane (1.0 mL). The solution was purged with Ar for 15 minutes, then placed in an oil bath at 90 °C for 16 hours. The polymerization was quenched by exposed the flask to air and bringing to room temperature. The polymer was recovered by precipitating into diethyl ether and drying *in vacuo* (0.260 g, = 49%). ^{1}H NMR (500 MHz, $CDCl_3$): δ 7.94-7.46 (b, 39H), 6.81-6.33 (b, 36H), 1.81-1.23 (b, 74H), 0.90 (t, 3H). $M_{n,\,NMR}$ = 3,600 g/mol, $M_{n,\,GPC\,(PS\,standards)}$ = 5,400 g/mol, Đ = 1.10.

Deprotection of polyvinylmethylbenzoate. To a 50 mL round bottom flask was added polyvinylmethylbenzoate (0.214 mg, 1.32 mmol), NaOH (1.58 g, 39.6 mmol), THF (10 mL), and water (5 mL). The mixture was stirred at 40 °C for 18 hours, after which the pH was adjusted to 1 with 5 M HCl, the precipitated polymer was collected by centrifugation, washed with excess water and dried *in vacuo* (134 mg, 68%). ^{1}H NMR (500 MHz, d_6-DMSO): δ 7.90-7.45 (b, 34H), 7.01-6.33 (b, 32H), 1.99-1.22 (b, 51H), 0.80 (t, 3H).

Materials characterization

Powder X-ray Diffraction (PXRD). PXRD data was collected at room temperature on a Bruker D8 Advance diffractometer running at 40 kV, 4 mA for Cu Kα (λ = 1.5418 Å), with a scan speed of 0.5 sec/step, a step size of 0.02° in 2θ, and a 2θ range of 5- 50° at room temperature. Sample holders used were zero-background Si plates (p- type, B-doped) from MTI Corp with well-type sample holders (depth = 0.5 mm).

Scanning Electron Microscopy (SEM). MMMs were placed on conductive carbon tape on a sample holder and coated using an Ir sputter-coating for 7 s. A FEI Quanta 250 scanning electron microscope was used for acquiring images using a 10 kV energy source under vacuum at a working distance of 10 mm. Examples of particle size determination are given in Figures S45-S48.

Gel-permeation chromatography (GPC). Gel-permeation chromatography of poly(vinylmethylbenzoate) was performed in DMF (0.7 mL/min) using a Malvern GPC equipped with D4000 single-pore column and D-6000M general-purpose mixed-bed weight divinylbenzene column connected in series to determine molecular weights and molecular weight distributions, Mw/Mn, of our polymers. The solutions were filtered through 0.4 μm PTFE membrane before being injected into either GPC instrument. Narrow poly (methyl methacrylate) (PMMA) was used as the calibration standard.

For aqueous GPC of PAA a Hitachi Chromaster system equipped with an RI detector and two 8 μm, mixed-M bed, 7.5 mm I.D. x 30 cm PL aquagel-OH columns in series (Agilent Technologies) were run in sequence using an isocratic method with a flow rate of 1.0mL/min in water (0.2M NaNO3 in 0.01M Na2HPO4, pH = 7.0).

N_2 Sorption Brunauer–Emmett–Teller (BET) Analysis. Approximately 50 mg of sample were placed in a tared sample tube and degassed at 105 °C on a Micromeritics ASAP 2020 Adsorption Analyzer until the outgas rate was <5 mmHg (12-48 h). Post-degas, the sample tube was weighed, and then N_2 sorption isotherm data was collected at 77 K on a Micromeritics ASAP 2020 Adsorption Analyzer using a volumetric technique.

Dynamic light scattering (DLS). Dynamic light scattering was performed on a Malvern Zetasizer ZS90, equipped with a 4 mW, 633 nm laser, operating at a scattering angle of 90°. Temporal fluctuations in raw light scattering data were analyzed via the second-order autocorrelation function

$$G^2(q,\tau) = \frac{\langle I(t)I(t+\tau)\rangle}{\langle I(t)\rangle^2}$$

where q is the scattering length vector, t is the time over which the autocorrelation function was calculated, τ is the sampling interval, and I is the intensity of scattered light. The scattering length vector q is calculated as

$$q = \frac{4\pi n}{\lambda}\sin\left(\frac{\theta}{2}\right)$$

where λ is the wavelength of incident light, n is the refractive index of the scattering medium, and θ is the detector angle. The second-order autocorrelation function was then analyzed via a cumulants analysis whereby an exponential decay is fitted to the form of

$$C(\tau) = e^{\left(-\bar{\Gamma}\left(\tau-\frac{\mu_2}{2!}\tau^2+\frac{\mu_3}{3!}\tau^3+\cdots\right)\right)}$$

where $C(\tau)$ is the baseline subtracted autocorrelation function, and the average decay rate, $\bar{\Gamma}$, and the second-order variance, μ_2, are obtained through a least squares optimization. The intensity weighted diffusion coefficient, D_t, can then be determined by

$$\bar{\Gamma} = D_t q^2$$

Finally, particle size can be calculated using the Stokes-Einstein equation

$$D_z = \frac{k_B T}{3\pi\eta D_t}$$

where k_B is the Boltzmann constant, T is the absolute temperature, and η is the solution viscosity. In addition to providing the particle size, the cumulants analysis is able to provide information about the size distributions of the particles through the polydispersity index, which is given by

$$PDI = \frac{\mu_2}{\bar{\Gamma}^2}$$

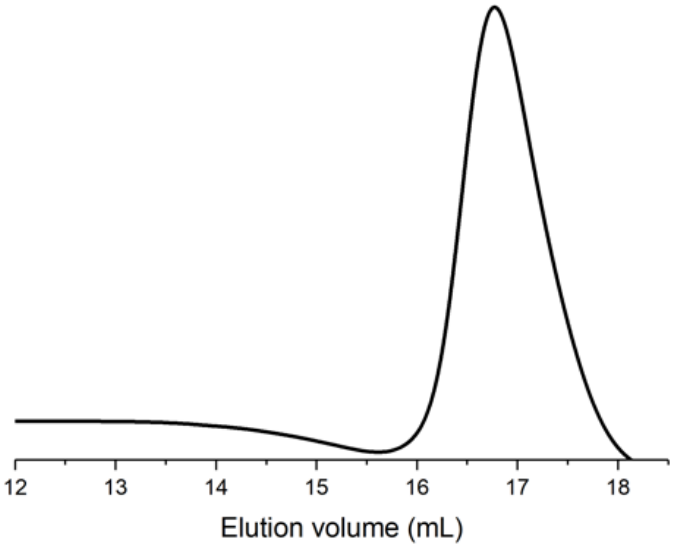

Figure S1. GPC chromatogram of PAA. $M_{n,}$ = 12,200 g/mol, Đ = 1.04, poly(ethylene glycol) standards.

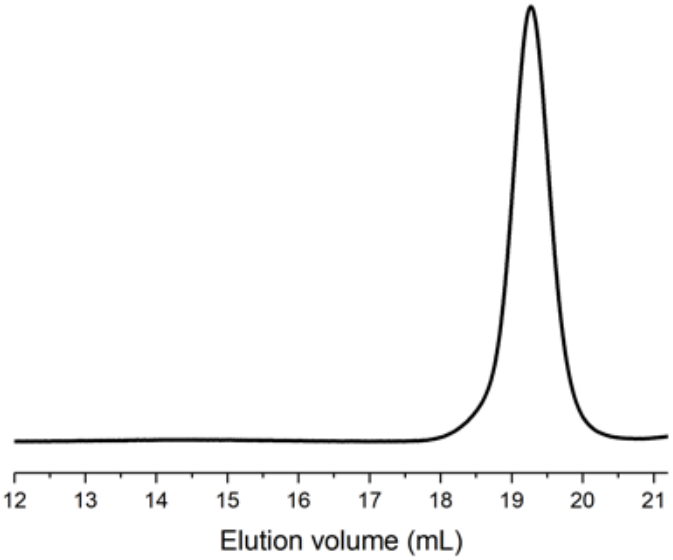

Figure S2. GPC chromatogram of polyvinylmethylbenzoate. $M_{n,\,GPC}$ = 5,400 g/mol, Đ = 1.10, polystyrene standards.

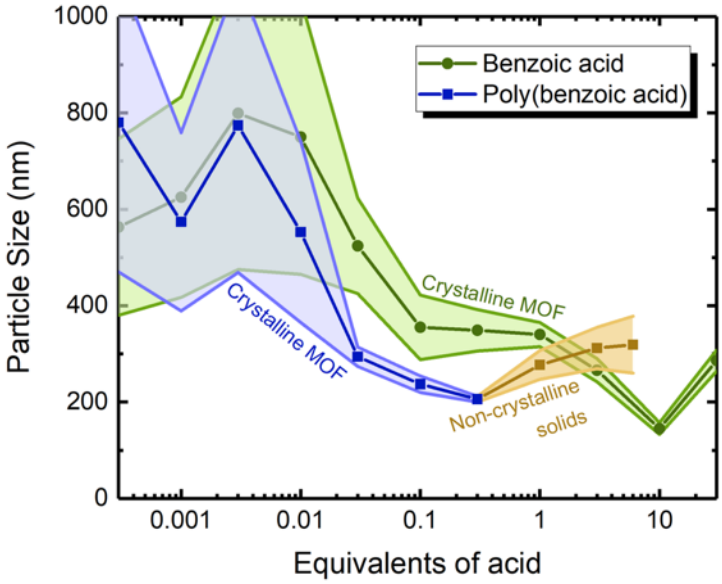

Figure S3. Particle size as a function of equivalents of PBA as measured by dynamic light scattering. Shaded areas represent the particle size distribution as determined by polydispersity index.

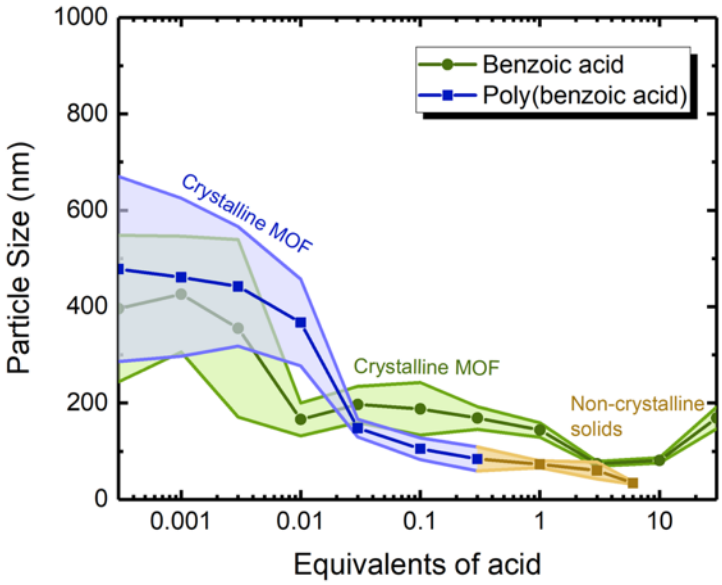

Figure S4. Particle size as a function of equivalents of PBA as measured by scanning electron microscopy. Shaded areas represent the particle size distribution as determined standard deviation.

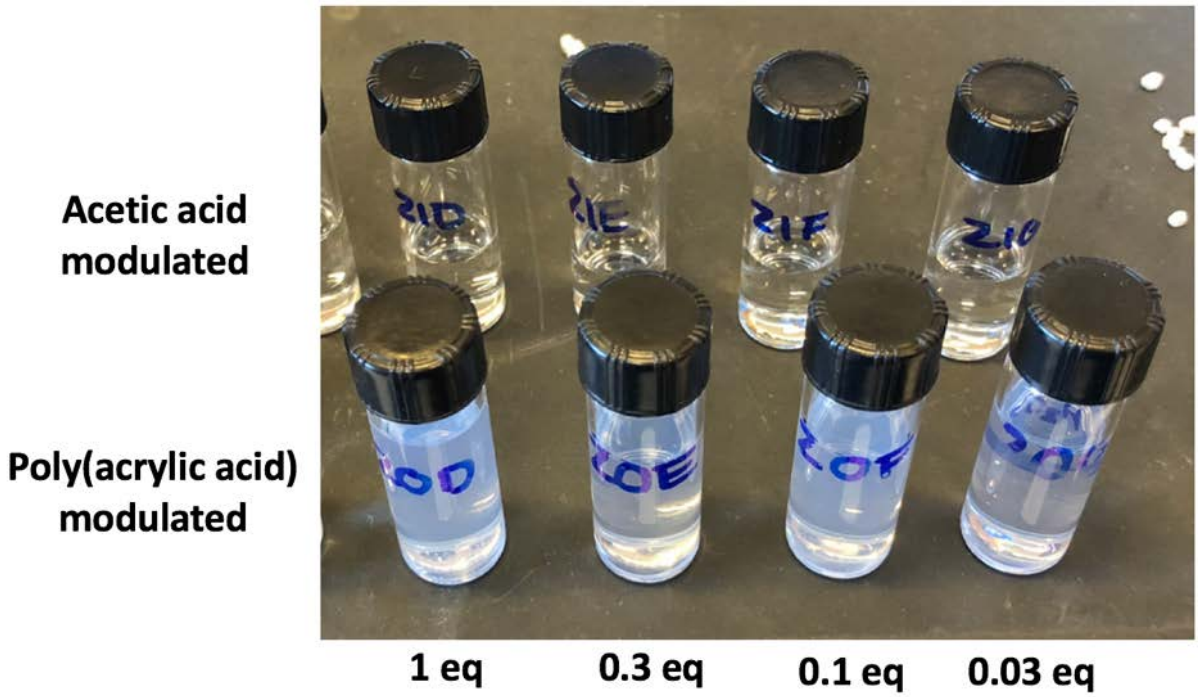

Figure S5. Demonstration of colloidal stability of UiO-66 particles (1 mg/mL in methanol) synthesized using AA modulator (top row) and PAA modulator (bottom row) at varying equivalences of acid after sitting undisturbed for 1 week.

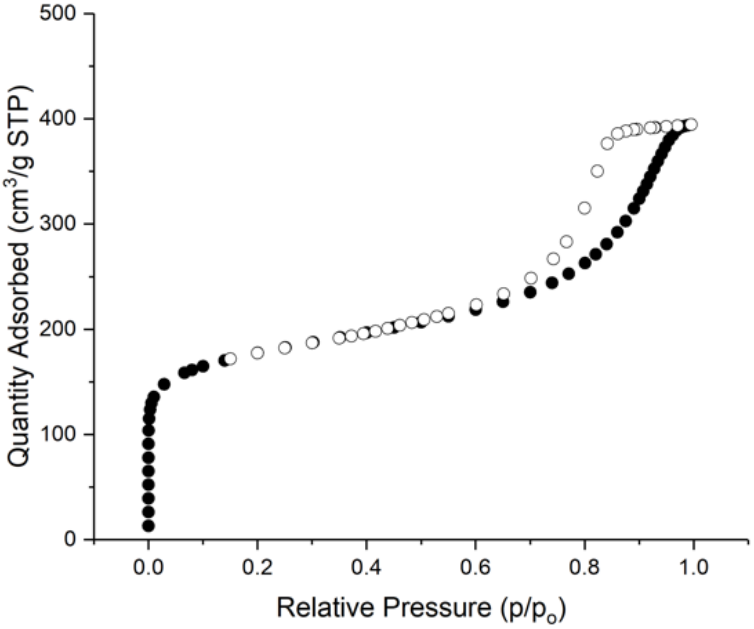

Figure S6. N_2 sorption isotherm of UiO-66 modulated with 1 equivalent of PAA (adsorption, closed circles; desorption open circles). BET surface area = 602 ± 52 m^2/g

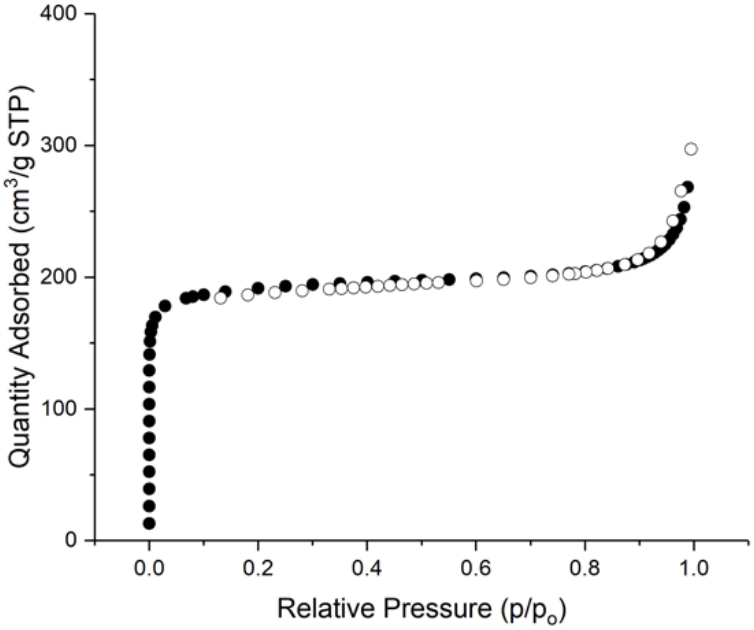

Figure S7. N_2 sorption isotherm of UiO-66 modulated with 0.03 equivalents of PAA (adsorption, closed circles; desorption open circles). BET surface area = 791 ± 41 m^2/g

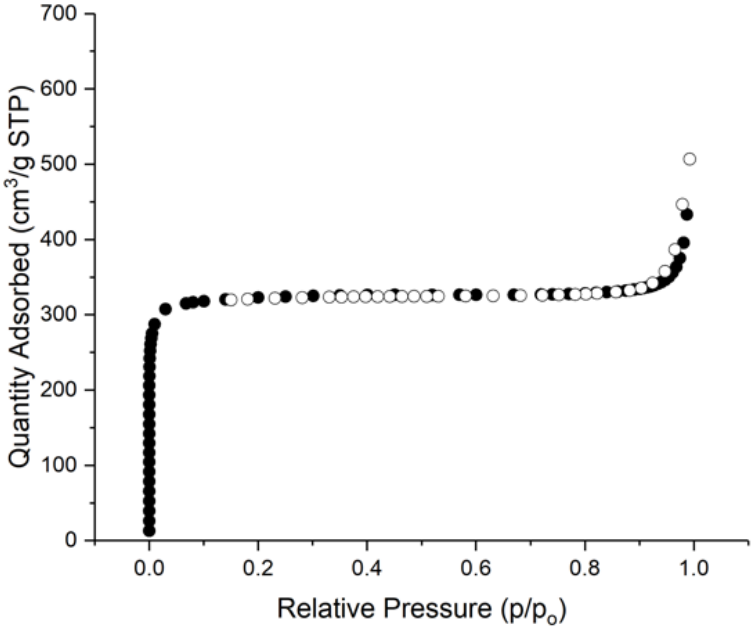

Figure S8. N_2 sorption isotherm of UiO-66 modulated with 30 equivalents of AA (adsorption, closed circles; desorption open circles). BET surface area = 1,229 ± 57 m^2/g

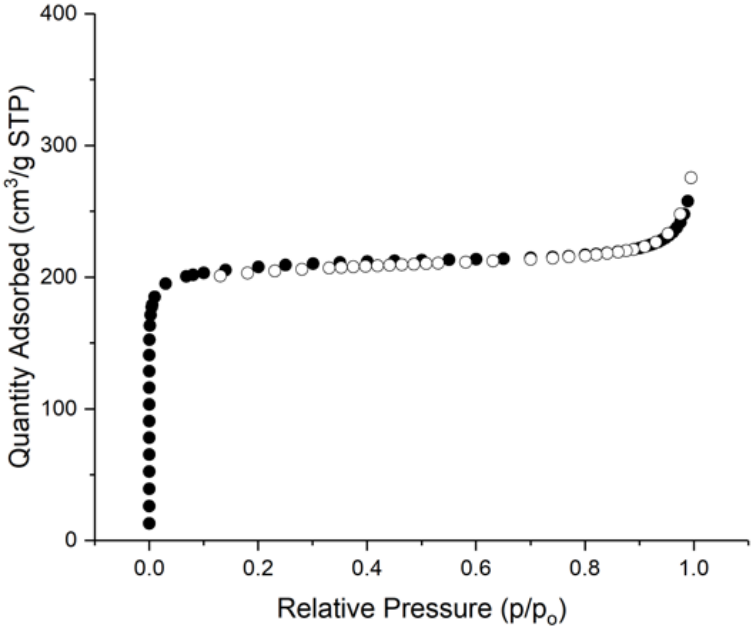

Figure S9. N_2 sorption isotherm of UiO-66 modulated with 30 equivalents of AA (adsorption, closed circles; desorption open circles). BET surface area = 716 ± 101 m^2/g

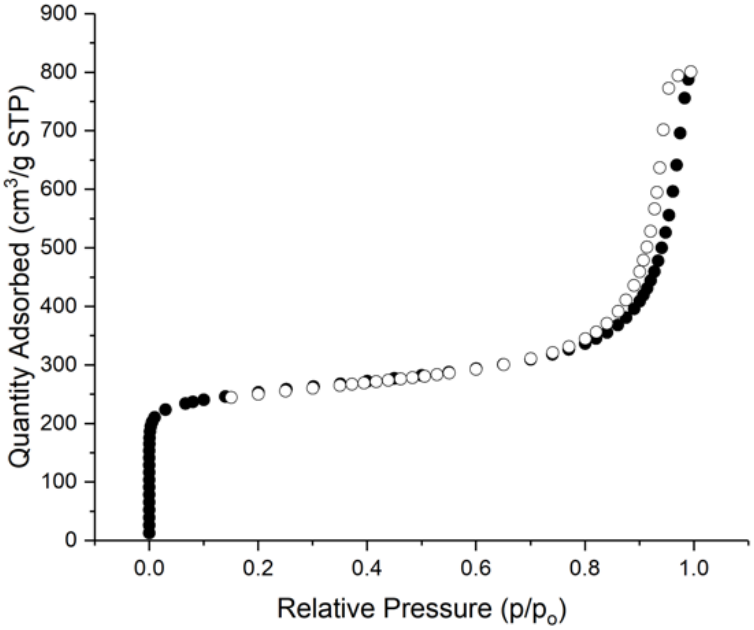

Figure S10. N_2 sorption isotherm of UiO-66 modulated with 0.3 equivalents of PBA (adsorption, closed circles; desorption open circles). BET surface area = 946 ± 13 m^2/g

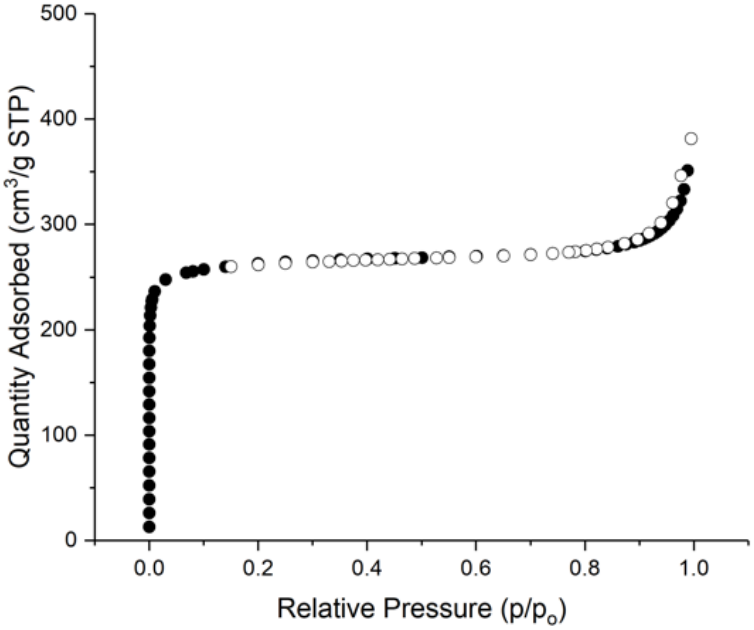

Figure S11. N_2 sorption isotherm of UiO-66 modulated with 0.03 equivalents of PBA (adsorption, closed circles; desorption open circles). BET surface area = 1,010 ± 25 m^2/g

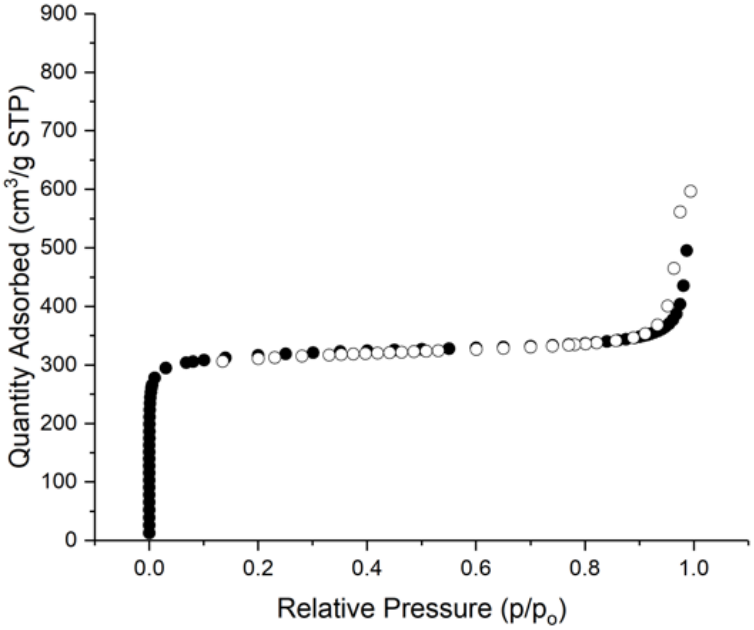

Figure S12. N_2 sorption isotherm of UiO-66 modulated with 10 equivalents of BA (adsorption, closed circles; desorption open circles). BET surface area = 1,046 ± 194 m^2/g

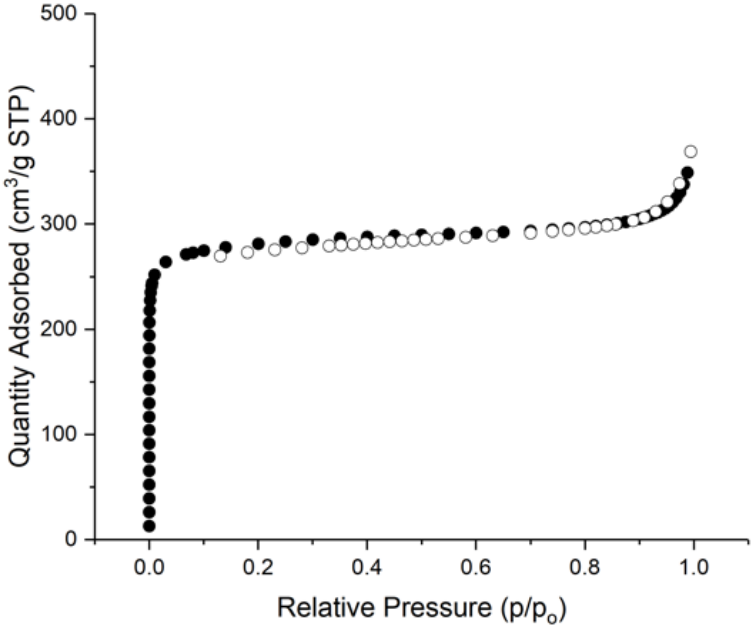

Figure S13. N_2 sorption isotherm of UiO-66 modulated with 0.3 equivalents of BA (adsorption, closed circles; desorption open circles). BET surface area = 1,018 ± 86 m^2/g

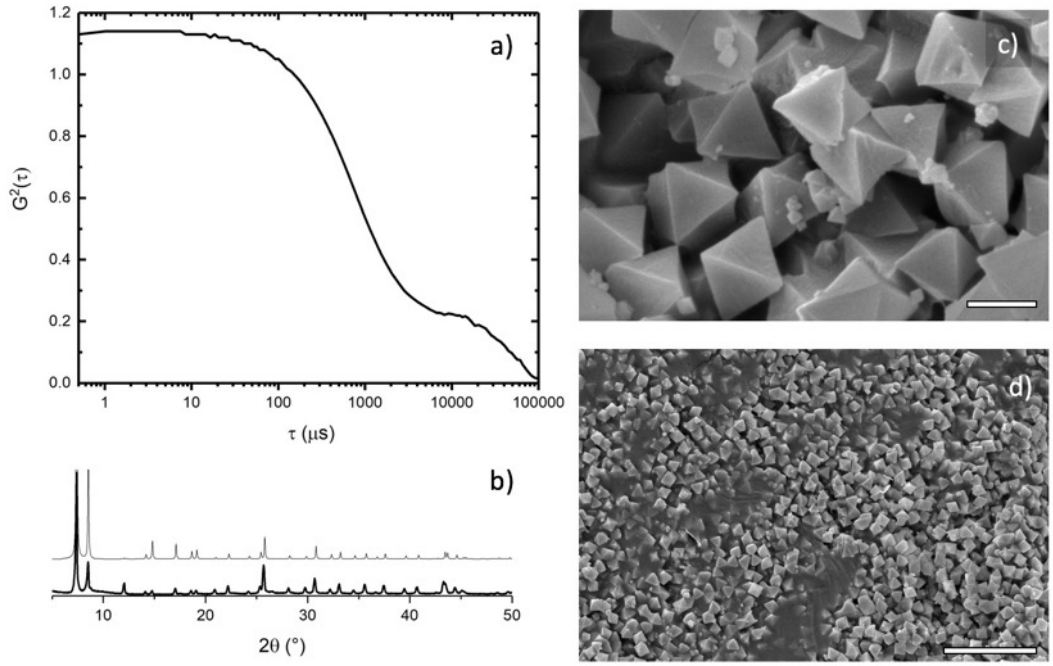

Figure S14. Characterization of UiO-66 modulated by 300 equivalents of AA: a) Dynamic light scattering correlation function; b) Powder X-ray diffraction pattern (simulated pattern above in gray); c, d) Scanning electron microscope images (scale bars = 500 nm, 5 μm, respectively).

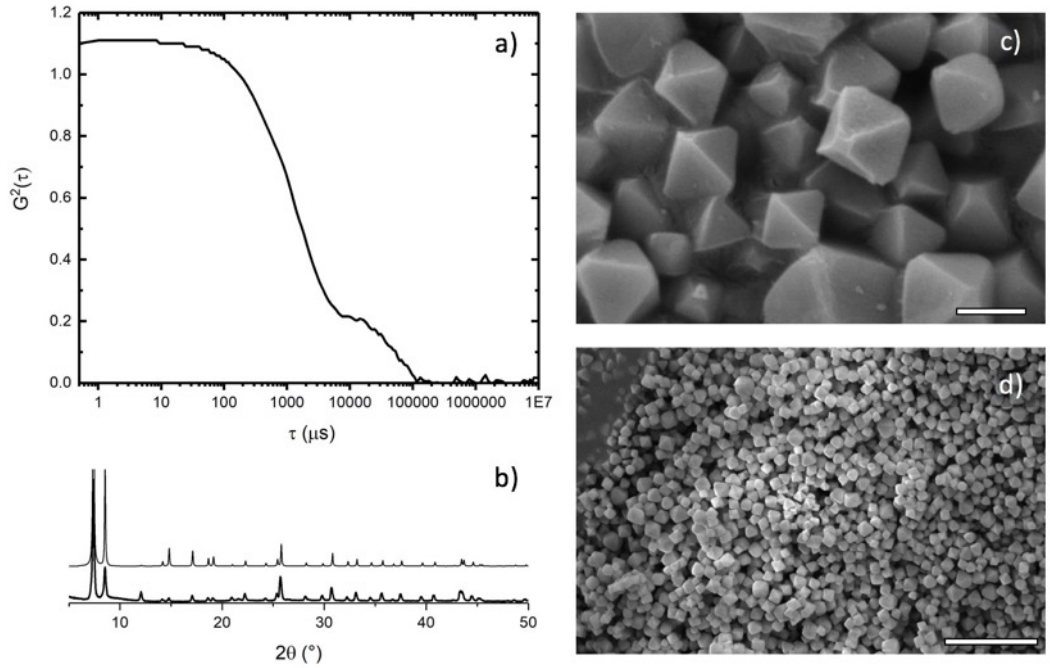

Figure S15. Characterization of UiO-66 modulated by 100 equivalents of AA: a) Dynamic light scattering correlation function; b) Powder X-ray diffraction pattern (simulated pattern above in gray); c, d) Scanning electron microscope images (scale bars = 500 nm, 5 μm, respectively).

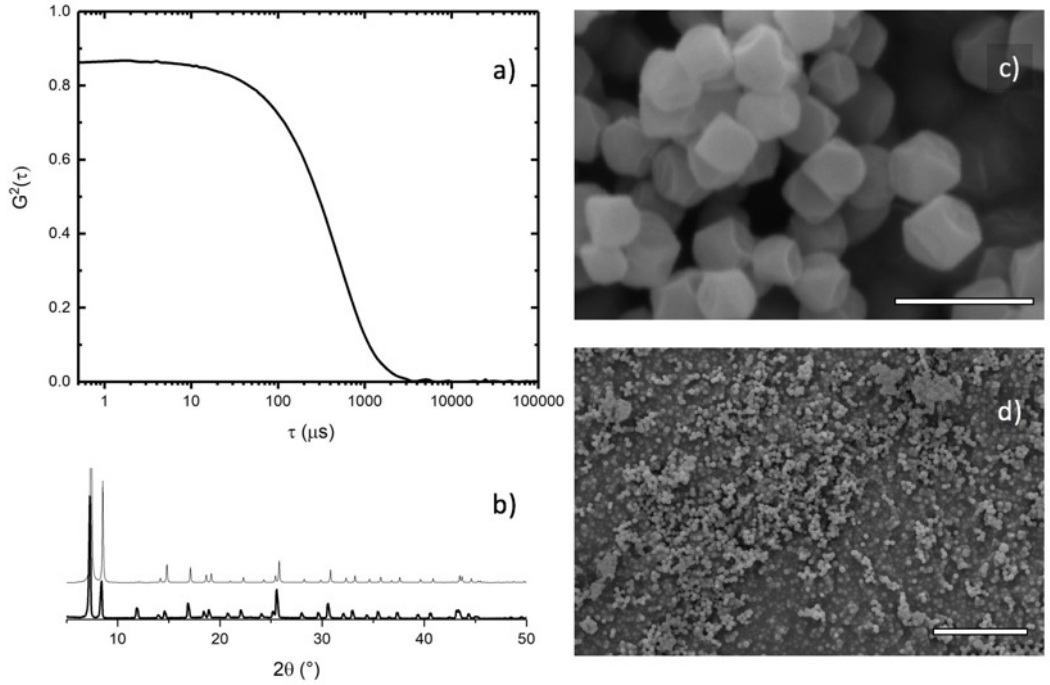

Figure S16. Characterization of UiO-66 modulated by 30 equivalents of AA: a) Dynamic light scattering correlation function; b) Powder X-ray diffraction pattern (simulated pattern above in gray); c, d) Scanning electron microscope images (scale bars = 500 nm, 5 μm, respectively).

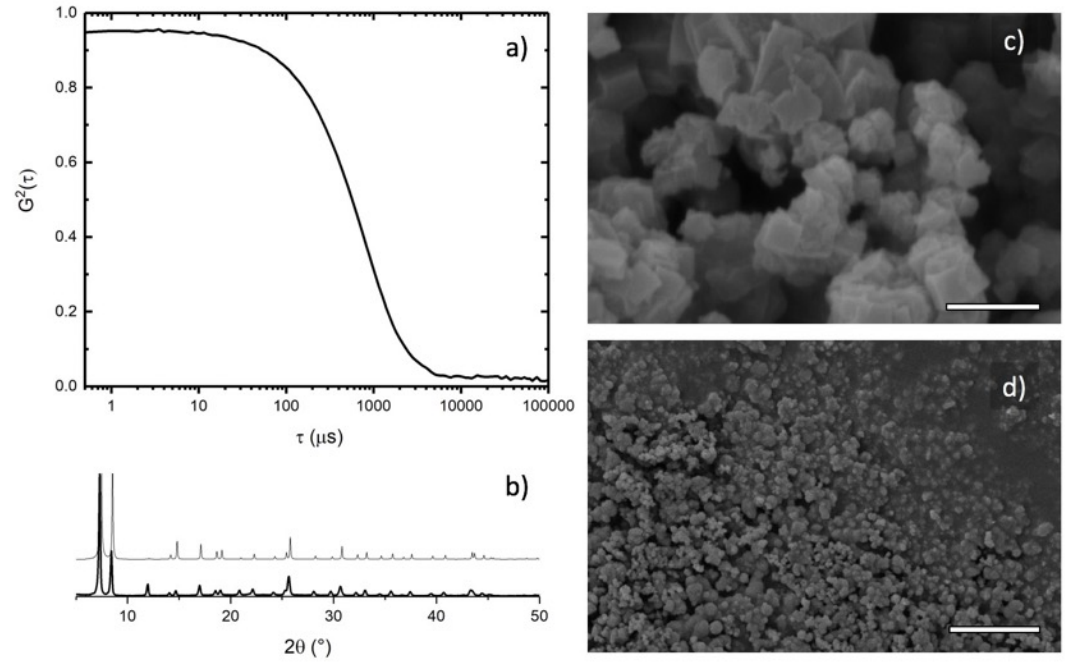

Figure S17. Characterization of UiO-66 modulated by 10 equivalents of AA: a) Dynamic light scattering correlation function; b) Powder X-ray diffraction pattern (simulated pattern above in gray); c, d) Scanning electron microscope images (scale bars = 500 nm, 5 μm, respectively).

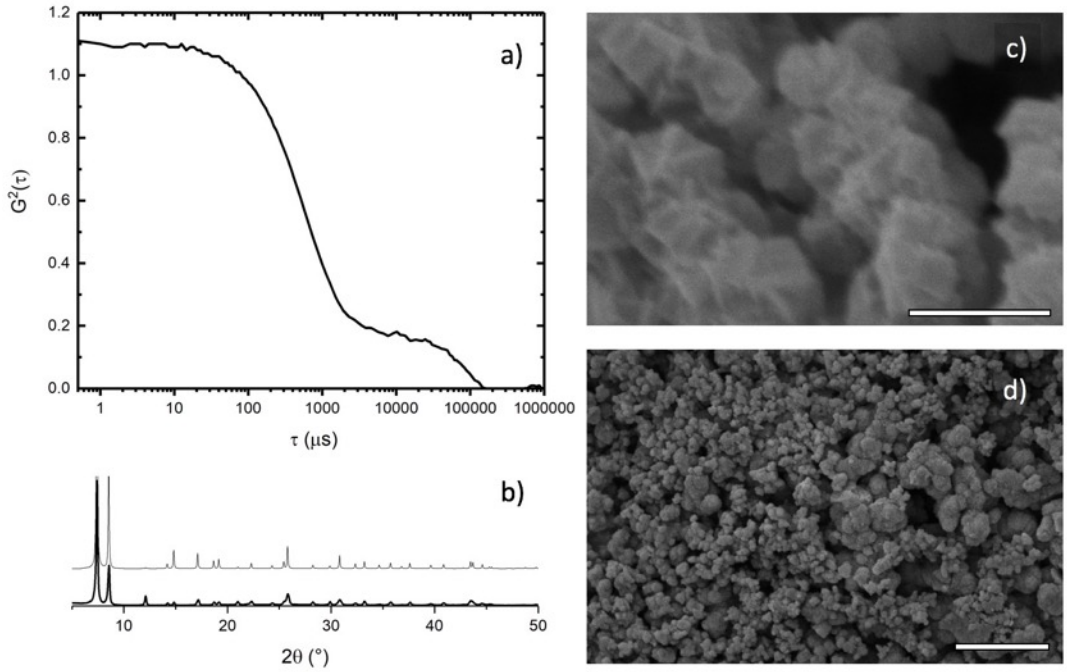

Figure S18. Characterization of UiO-66 modulated by 3 equivalents of AA: a) Dynamic light scattering correlation function; b) Powder X-ray diffraction pattern (simulated pattern above in gray); c, d) Scanning electron microscope images (scale bars = 500 nm, 5 μm, respectively).

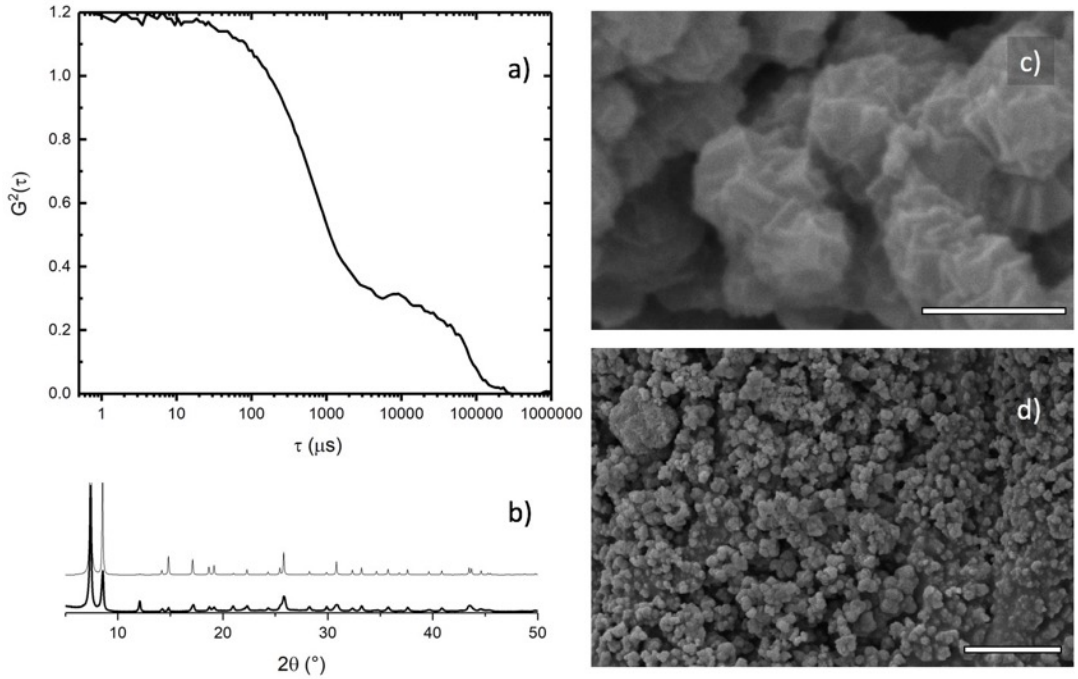

Figure S19. Characterization of UiO-66 modulated by 1 equivalent of AA: a) Dynamic light scattering correlation function; b) Powder X-ray diffraction pattern (simulated pattern above in gray); c, d) Scanning electron microscope images (scale bars = 500 nm, 5 μm, respectively).

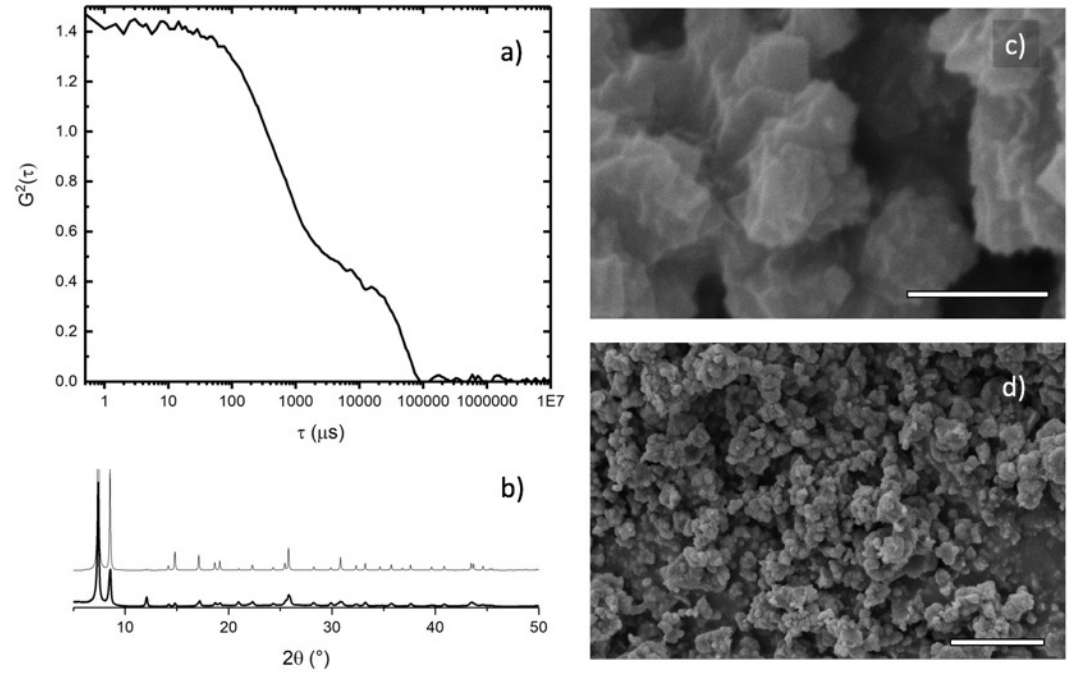

Figure S20. Characterization of UiO-66 modulated by 0.3 equivalents of AA: a) Dynamic light scattering correlation function; b) Powder X-ray diffraction pattern (simulated pattern above in gray); c, d) Scanning electron microscope images (scale bars = 500 nm, 5 μm, respectively).

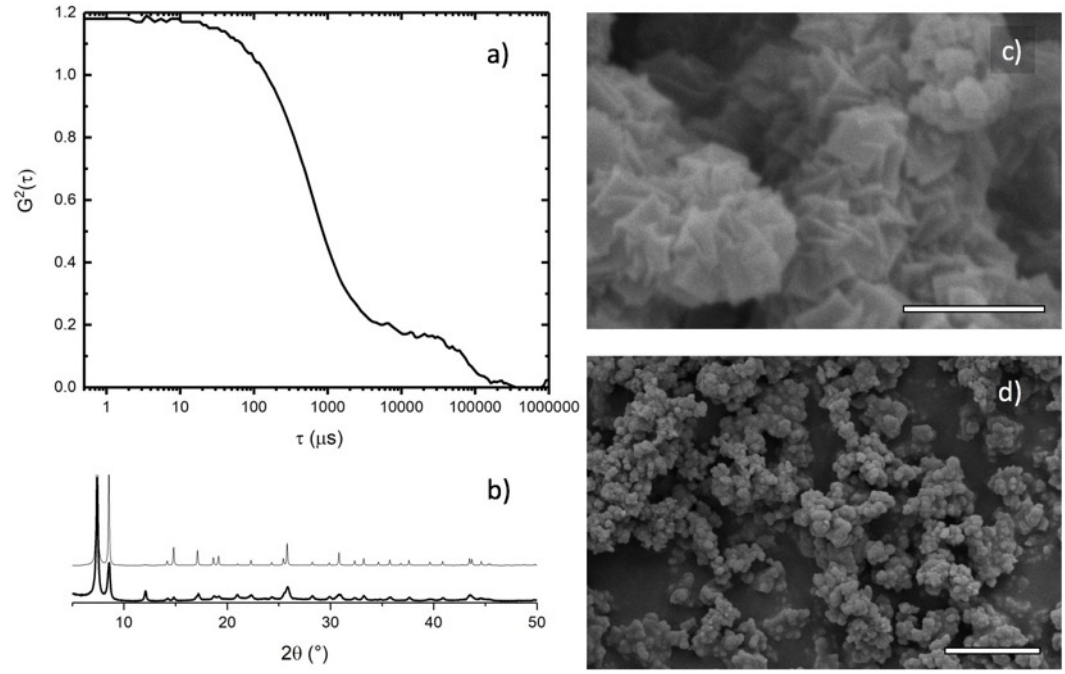

Figure S21. Characterization of UiO-66 modulated by 0.1 equivalents of AA: a) Dynamic light scattering correlation function; b) Powder X-ray diffraction pattern (simulated pattern above in gray); c, d) Scanning electron microscope images (scale bars = 500 nm, 5 μm, respectively).

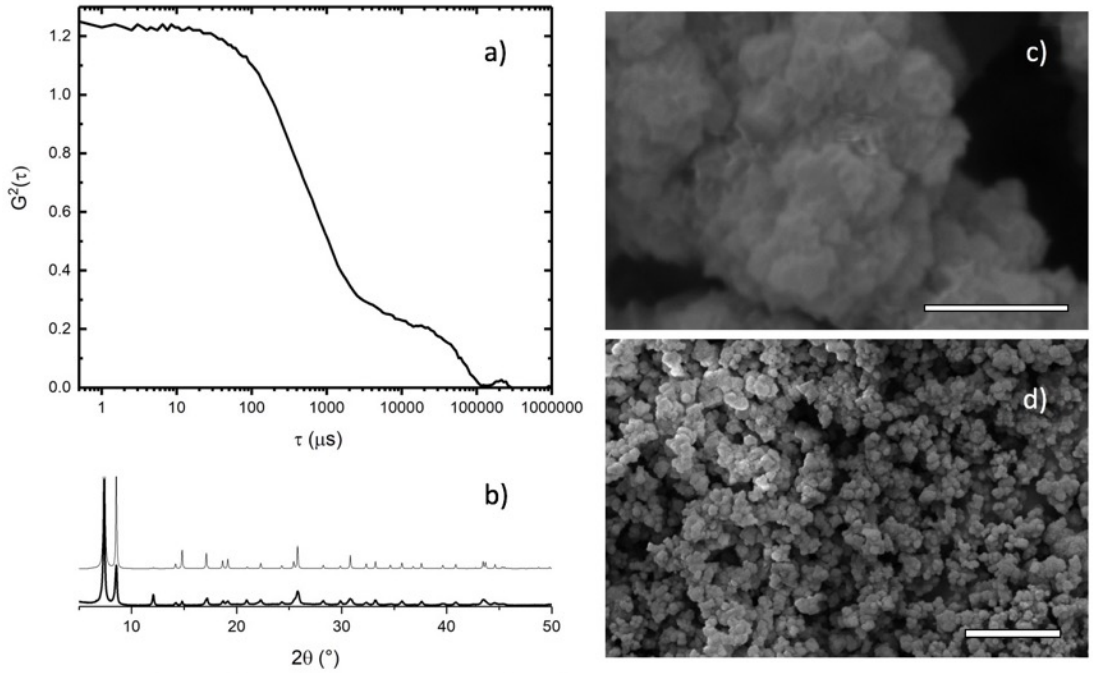

Figure S22. Characterization of UiO-66 modulated by 0.03 equivalents of AA: a) Dynamic light scattering correlation function; b) Powder X-ray diffraction pattern (simulated pattern above in gray); c, d) Scanning electron microscope images (scale bars = 500 nm, 5 μm, respectively).

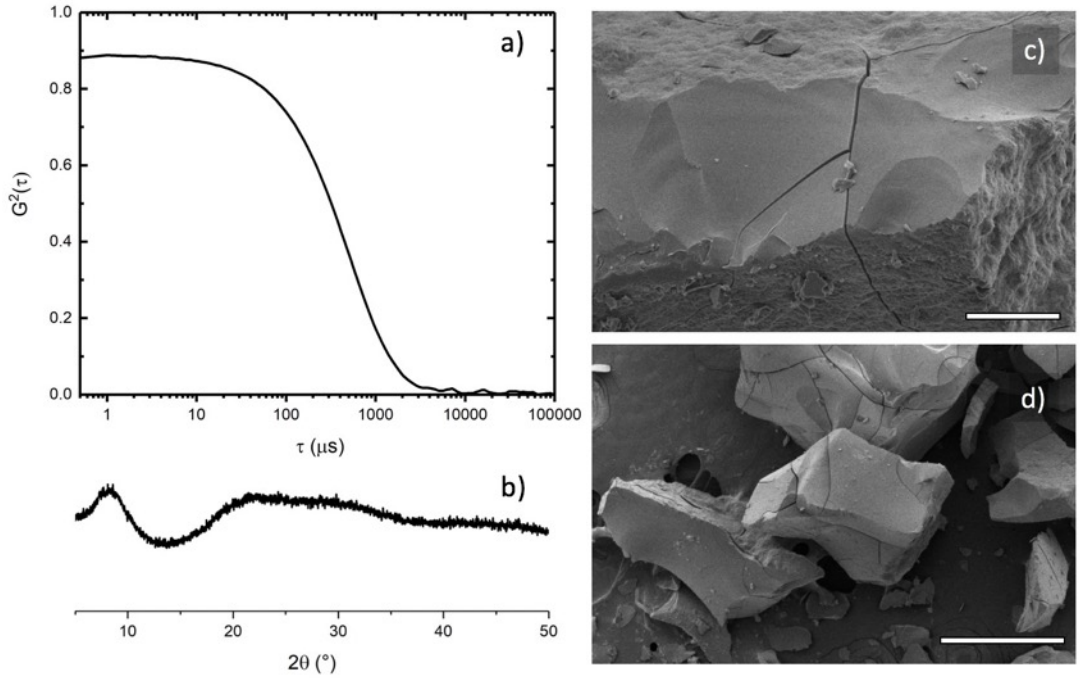

Figure S23. Characterization of UiO-66 modulated by 3 equivalents of PAA: a) Dynamic light scattering correlation function; b) Powder X-ray diffraction pattern (simulated pattern above in gray); c, d) Scanning electron microscope images (scale bars = 20 μm, 400 μm, respectively).

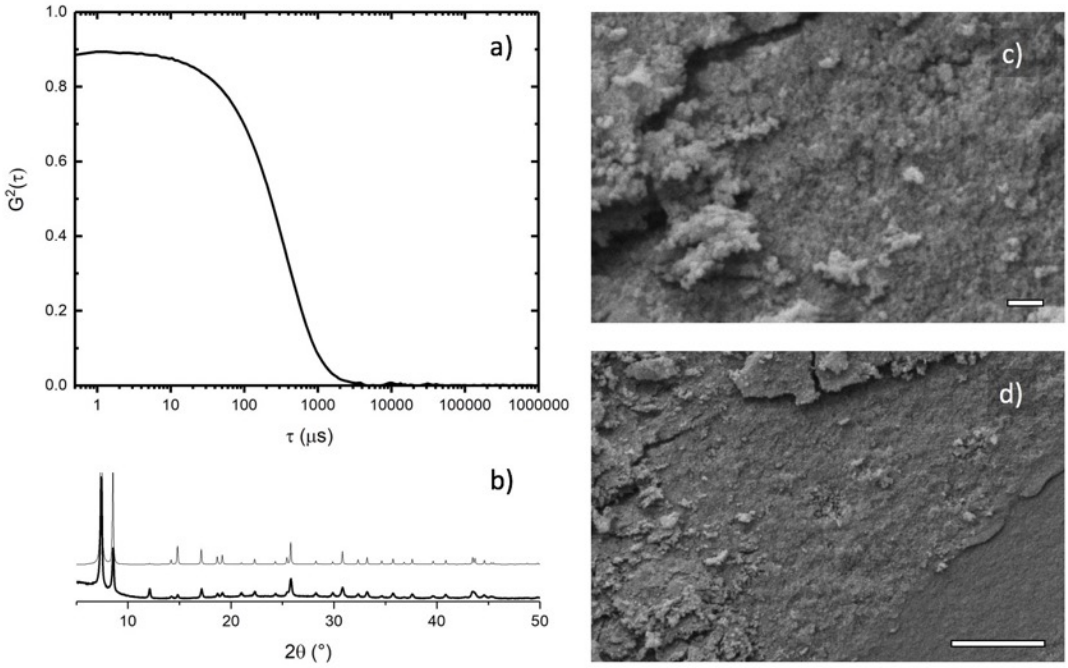

Figure S24. Characterization of UiO-66 modulated by 1 equivalent of PAA: a) Dynamic light scattering correlation function; b) Powder X-ray diffraction pattern (simulated pattern above in gray); c, d) Scanning electron microscope images (scale bars = 500 nm, 5 μm, respectively).

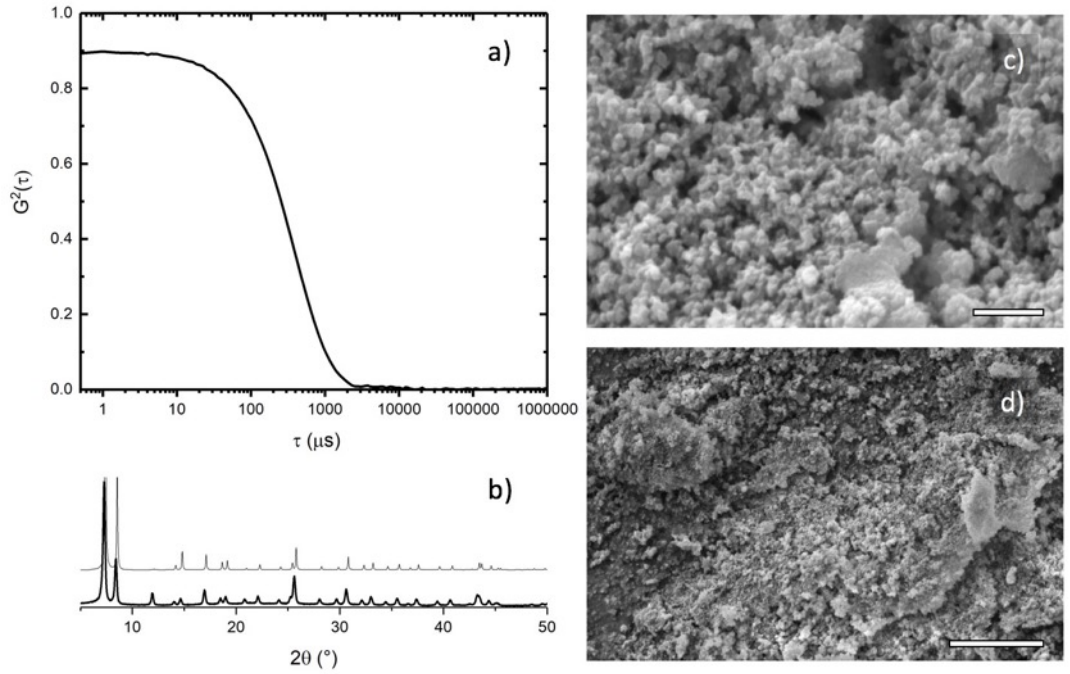

Figure S25. Characterization of UiO-66 modulated by 0.3 equivalents of PAA: a) Dynamic light scattering correlation function; b) Powder X-ray diffraction pattern (simulated pattern above in gray); c, d) Scanning electron microscope images (scale bars = 500 nm, 5 μm, respectively).

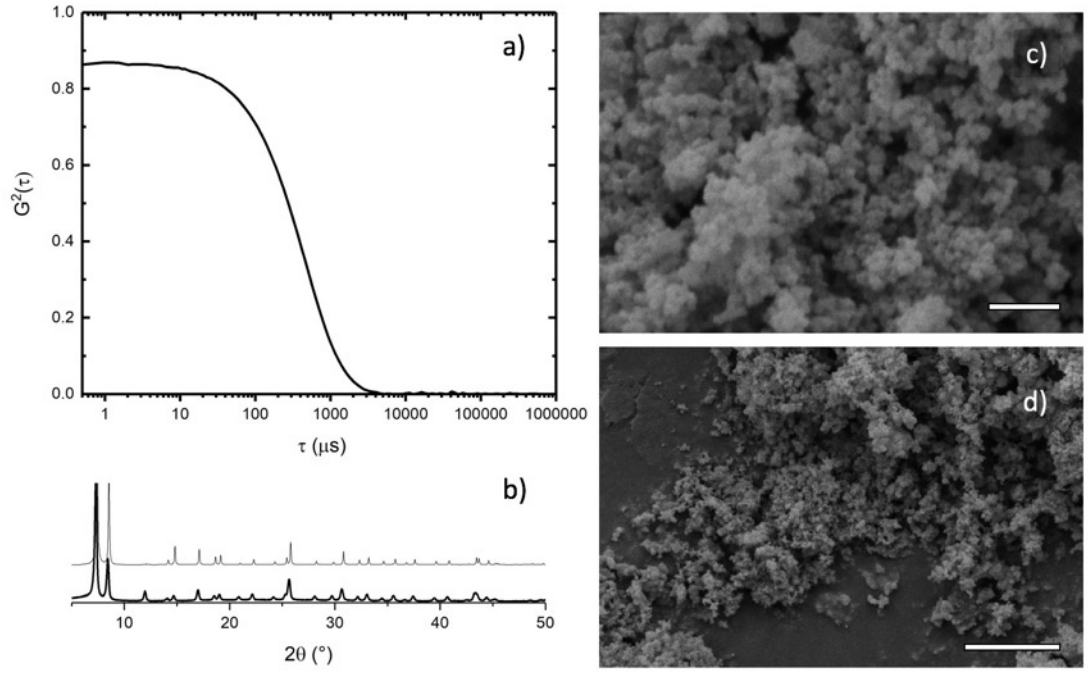

Figure S26. Characterization of UiO-66 modulated by 0.1 equivalents of PAA: a) Dynamic light scattering correlation function; b) Powder X-ray diffraction pattern (simulated pattern above in gray); c, d) Scanning electron microscope images (scale bars = 500 nm, 5 μm, respectively).

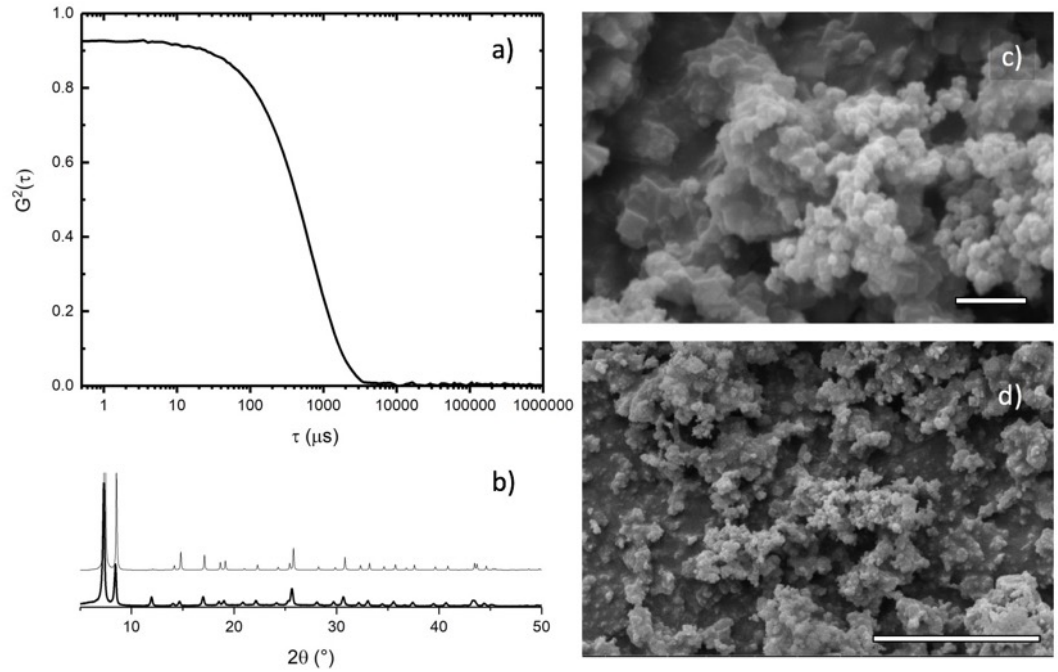

Figure S27. Characterization of UiO-66 modulated by 0.03 equivalents of PAA: a) Dynamic light scattering correlation function; b) Powder X-ray diffraction pattern (simulated pattern above in gray); c, d) Scanning electron microscope images (scale bars = 500 nm, 5 μm, respectively).

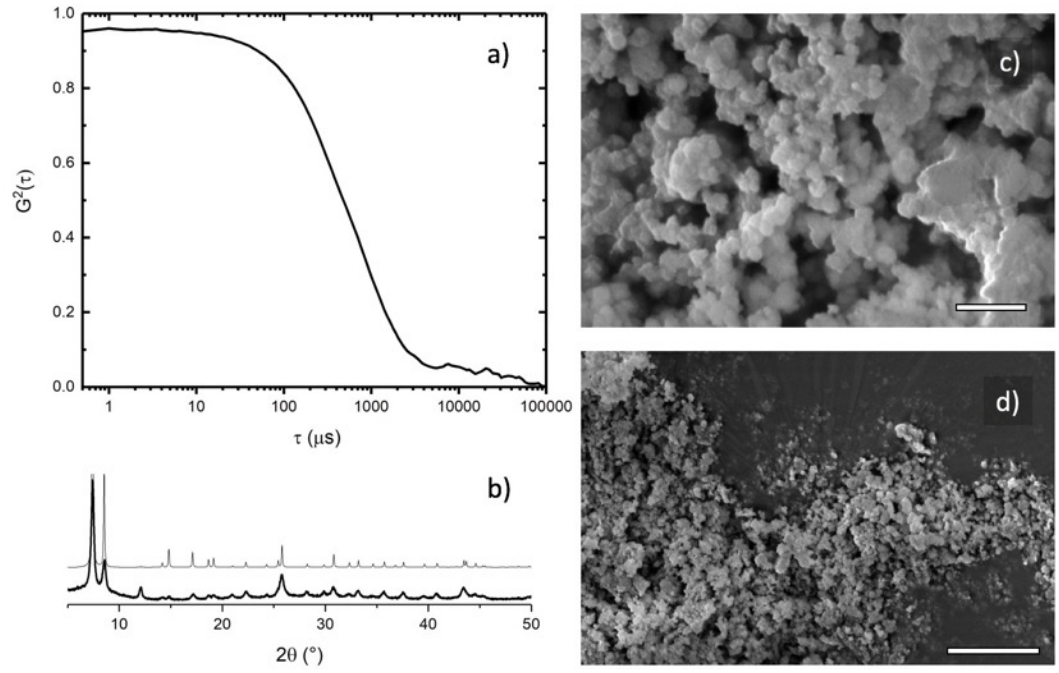

Figure S28. Characterization of UiO-66 modulated by 0.01 equivalents of PAA: a) Dynamic light scattering correlation function; b) Powder X-ray diffraction pattern (simulated pattern above in gray); c, d) Scanning electron microscope images (scale bars = 500 nm, 5 μm, respectively).

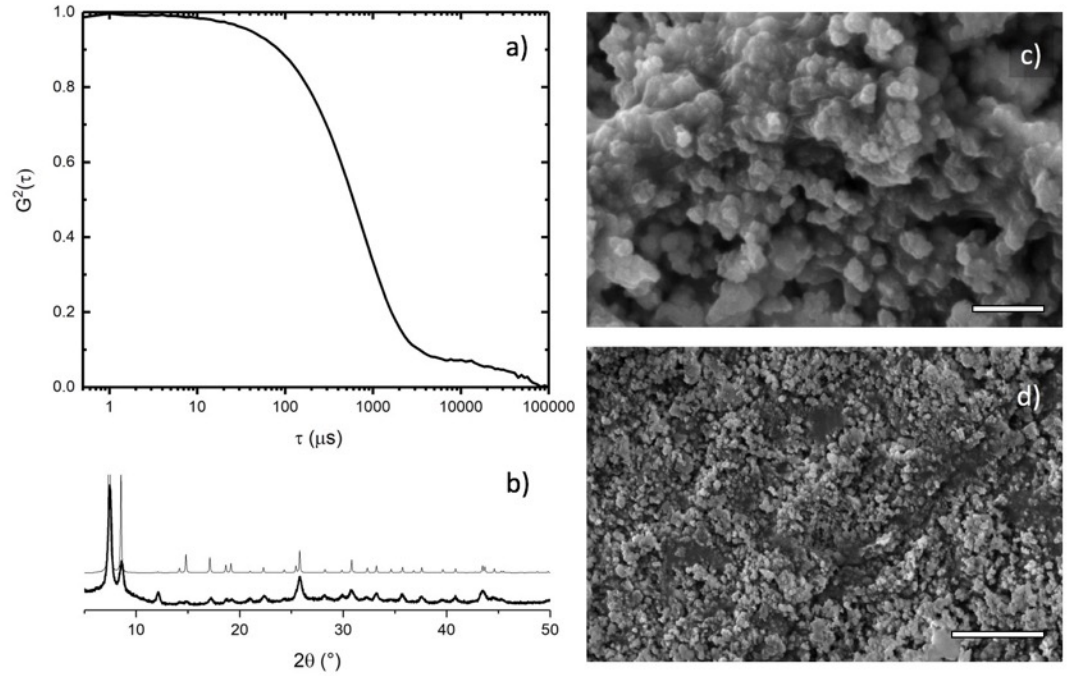

Figure S29. Characterization of UiO-66 modulated by 0.003 equivalents of PAA: a) Dynamic light scattering correlation function; b) Powder X-ray diffraction pattern (simulated pattern above in gray); c, d) Scanning electron microscope images (scale bars = 500 nm, 5 μm, respectively).

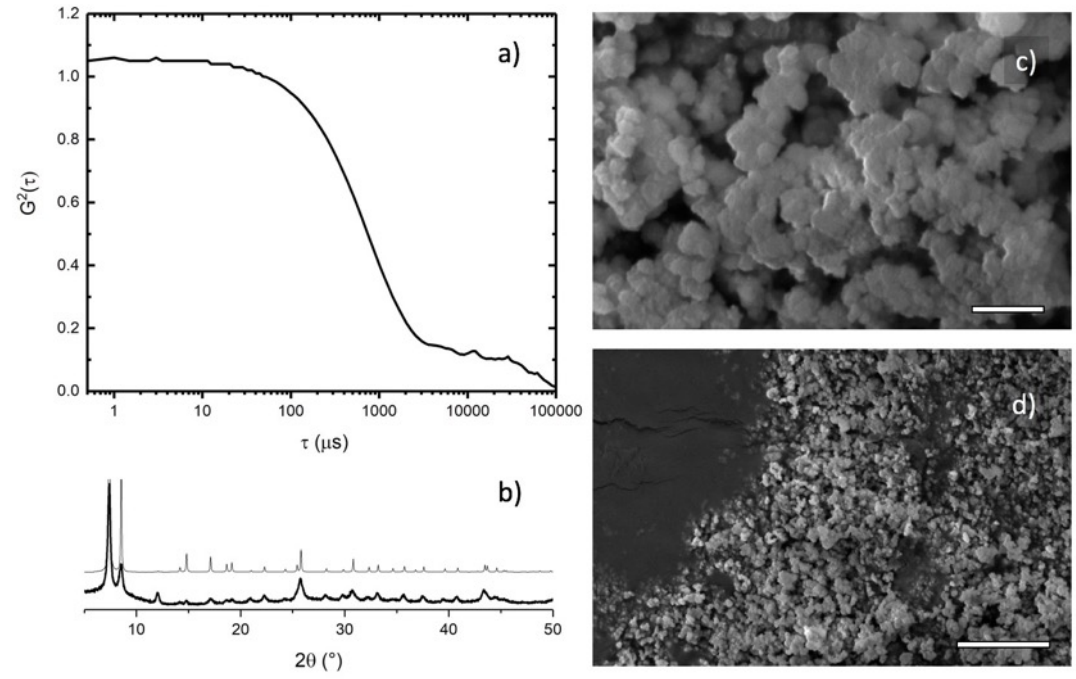

Figure S30. Characterization of UiO-66 modulated by 0.001 equivalents of PAA: a) Dynamic light scattering correlation function; b) Powder X-ray diffraction pattern (simulated pattern above in gray); c, d) Scanning electron microscope images (scale bars = 500 nm, 5 μm, respectively).

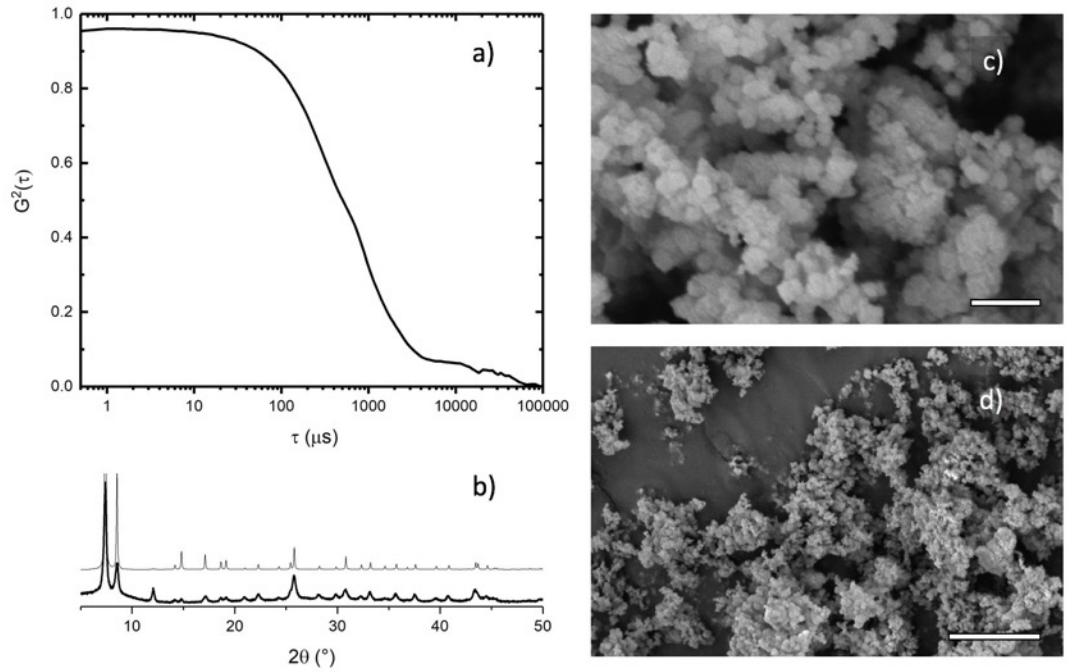

Figure S31. Characterization of UiO-66 modulated by 0.0003 equivalents of PAA: a) Dynamic light scattering correlation function; b) Powder X-ray diffraction pattern (simulated pattern above in gray); c, d) Scanning electron microscope images (scale bars = 500 nm, 5 μm, respectively).

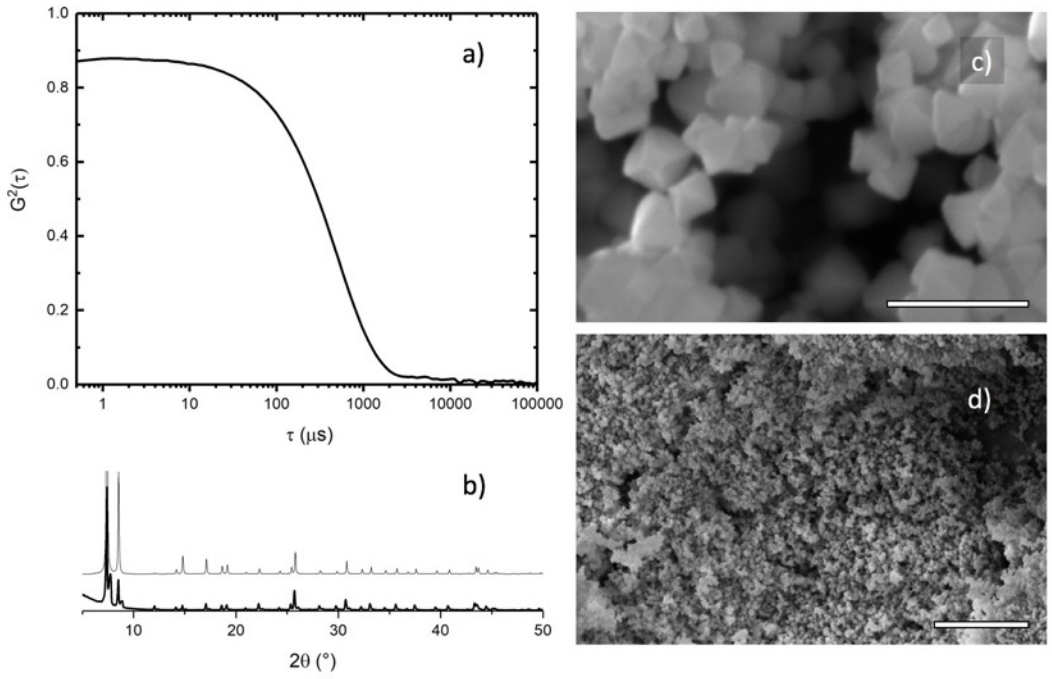

Figure S32. Characterization of UiO-66 modulated by 30 equivalents of BA: a) Dynamic light scattering correlation function; b) Powder X-ray diffraction pattern (simulated pattern above in gray); c, d) Scanning electron microscope images (scale bars = 500 nm, 5 μm, respectively).

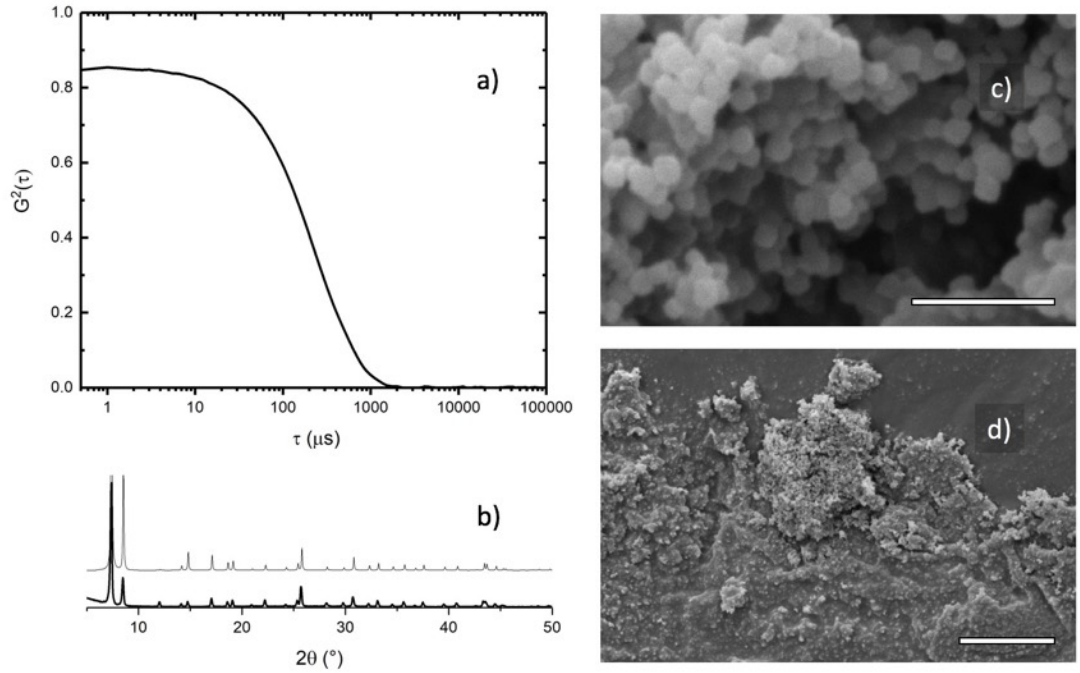

Figure S33. Characterization of UiO-66 modulated by 10 equivalents of BA: a) Dynamic light scattering correlation function; b) Powder X-ray diffraction pattern (simulated pattern above in gray); c, d) Scanning electron microscope images (scale bars = 500 nm, 5 μm, respectively).

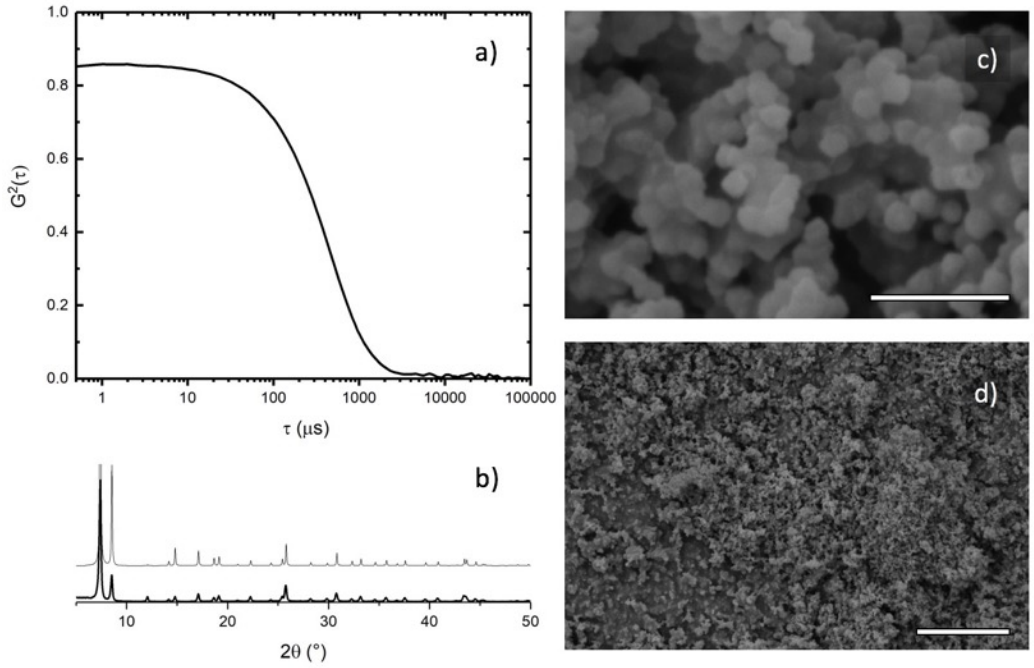

Figure S34. Characterization of UiO-66 modulated by 3 equivalents of BA: a) Dynamic light scattering correlation function; b) Powder X-ray diffraction pattern (simulated pattern above in gray); c, d) Scanning electron microscope images (scale bars = 500 nm, 5 μm, respectively).

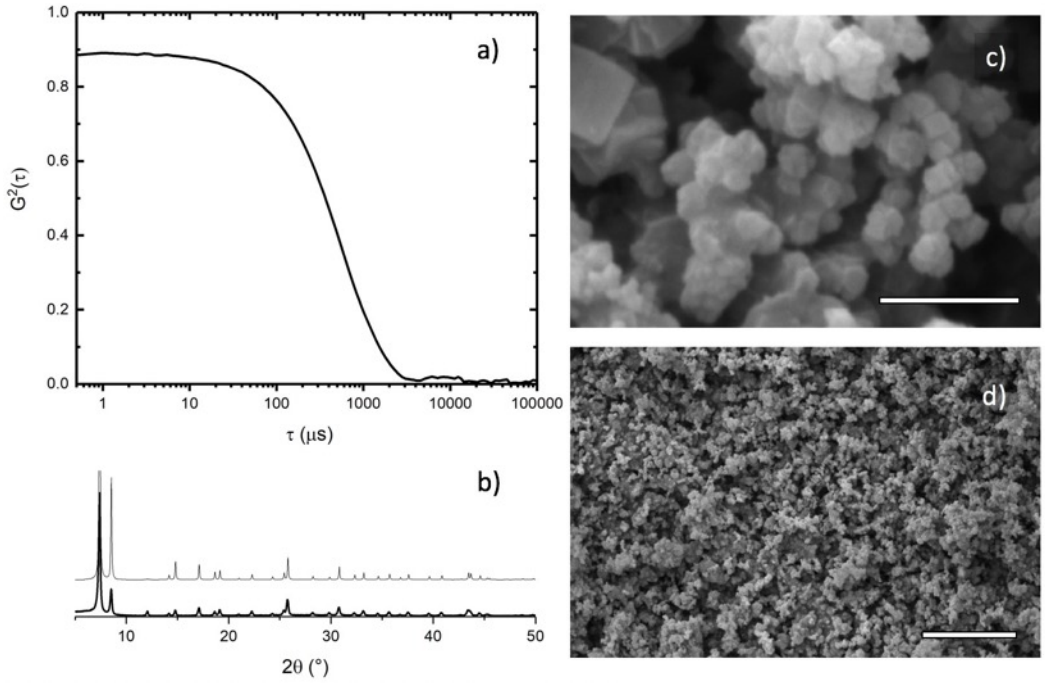

Figure S35. Characterization of UiO-66 modulated by 1 equivalent of BA: a) Dynamic light scattering correlation function; b) Powder X-ray diffraction pattern (simulated pattern above in gray); c, d) Scanning electron microscope images (scale bars = 500 nm, 5 μm, respectively).

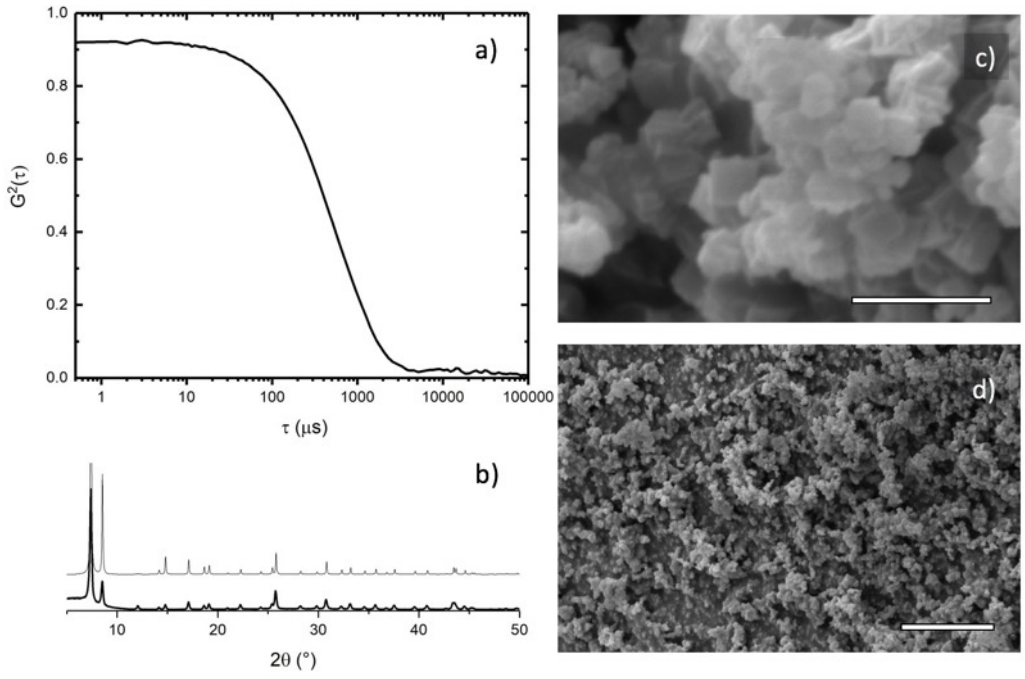

Figure S36. Characterization of UiO-66 modulated by 0.3 equivalents of BA: a) Dynamic light scattering correlation function; b) Powder X-ray diffraction pattern (simulated pattern above in gray); c, d) Scanning electron microscope images (scale bars = 500 nm, 5 μm, respectively).

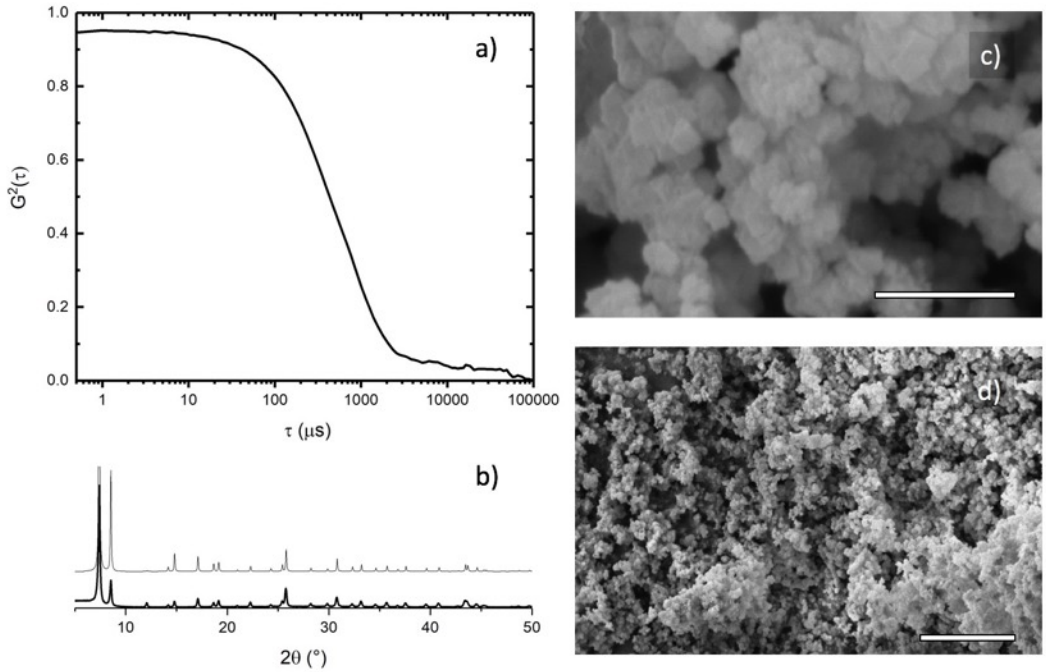

Figure S37. Characterization of UiO-66 modulated by 0.1 equivalents of BA: a) Dynamic light scattering correlation function; b) Powder X-ray diffraction pattern (simulated pattern above in gray); c, d) Scanning electron microscope images (scale bars = 500 nm, 5 μm, respectively).

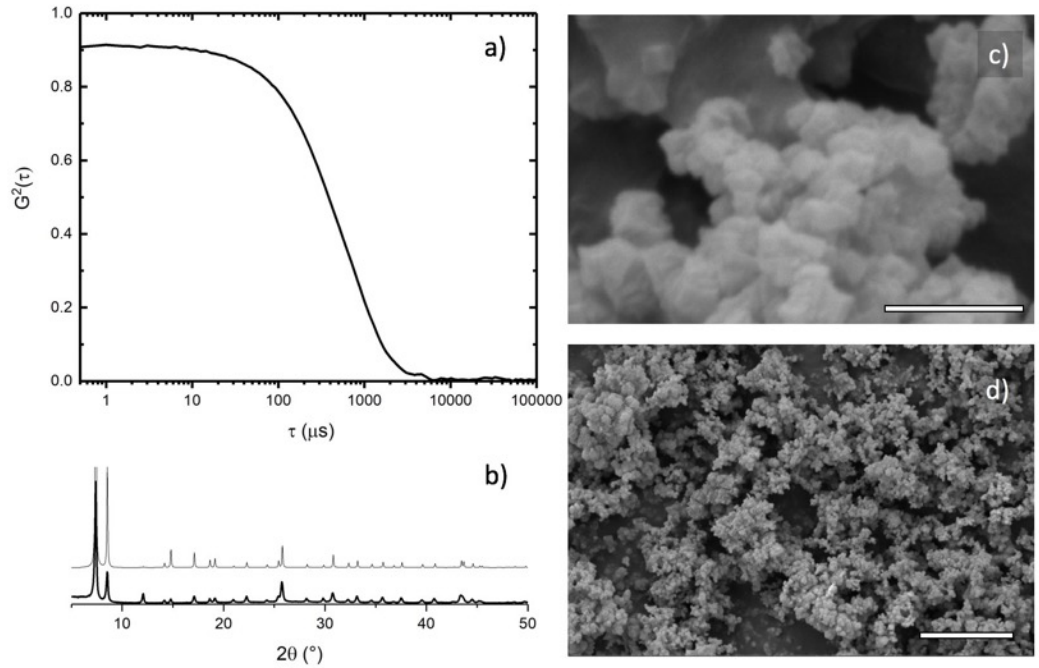

Figure S38. Characterization of UiO-66 modulated by 0.03 equivalents of BA: a) Dynamic light scattering correlation function; b) Powder X-ray diffraction pattern (simulated pattern above in gray); c, d) Scanning electron microscope images (scale bars = 500 nm, 5 μm, respectively).

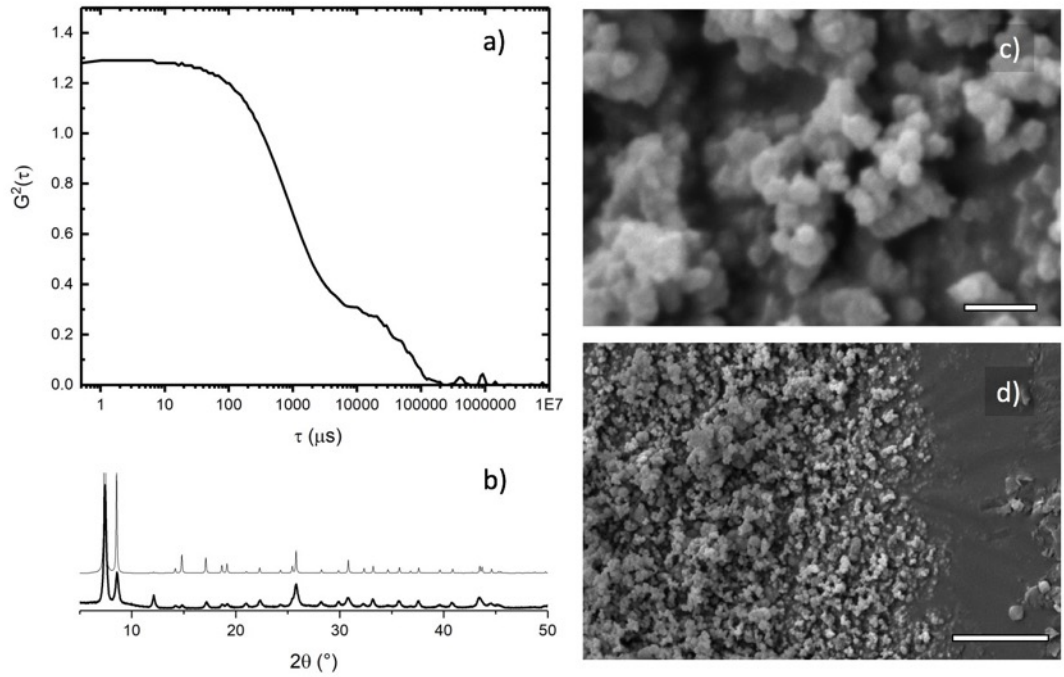

Figure S39. Characterization of UiO-66 modulated by 0.01 equivalents of BA: a) Dynamic light scattering correlation function; b) Powder X-ray diffraction pattern (simulated pattern above in gray); c, d) Scanning electron microscope images (scale bars = 500 nm, 5 μm, respectively).

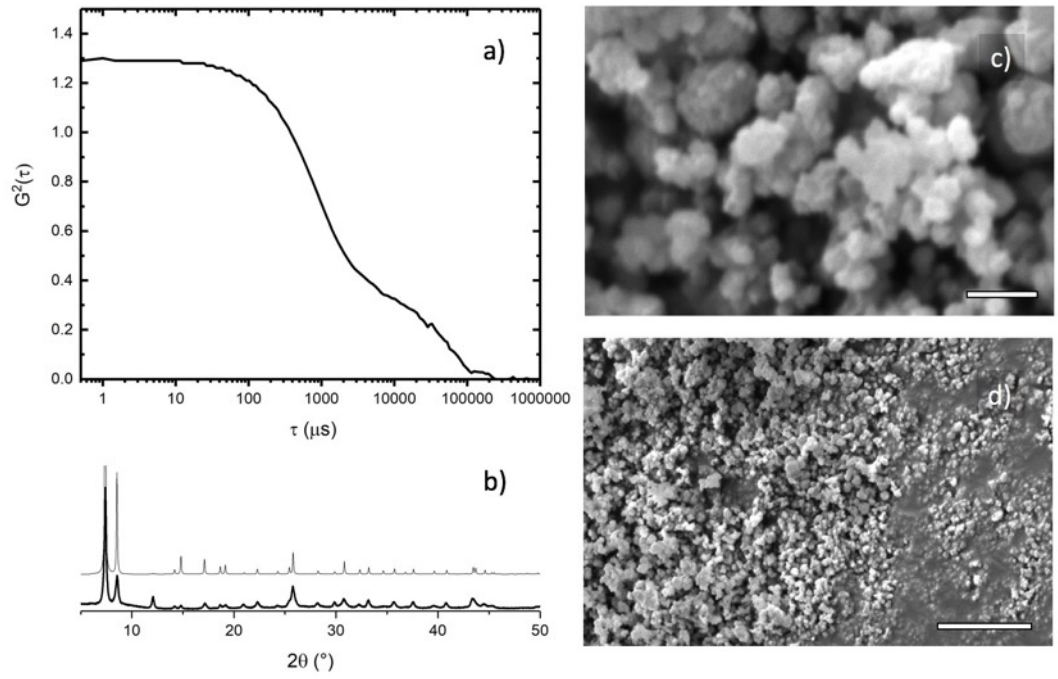

Figure S40. Characterization of UiO-66 modulated by 0.003 equivalents of BA: a) Dynamic light scattering correlation function; b) Powder X-ray diffraction pattern (simulated pattern above in gray); c, d) Scanning electron microscope images (scale bars = 500 nm, 5 μm, respectively).

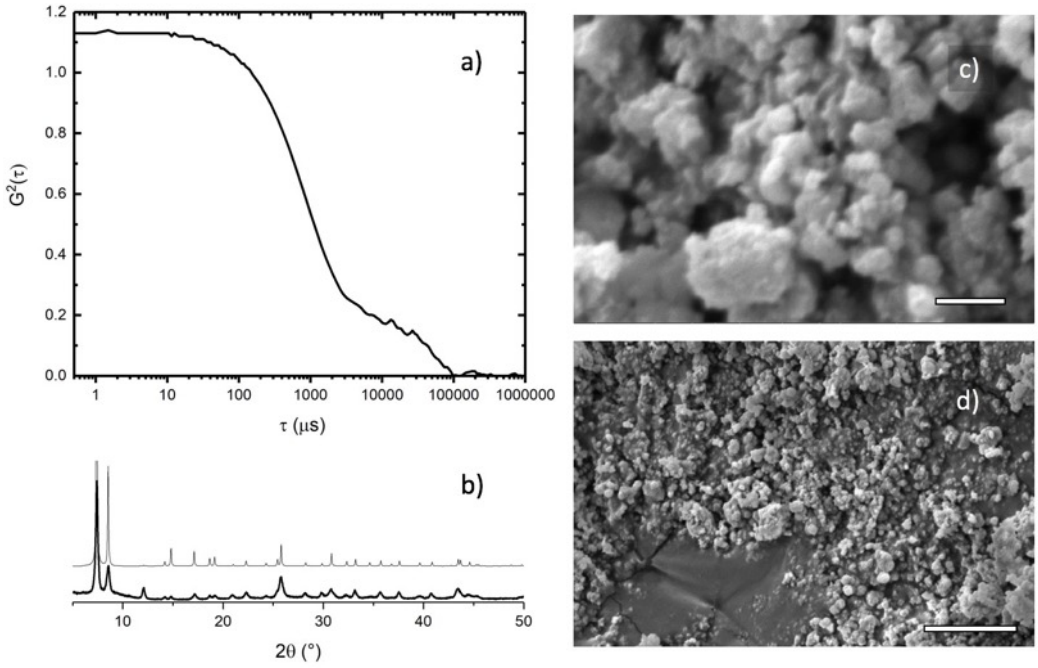

Figure S41. Characterization of UiO-66 modulated by 0.001 equivalents of BA: a) Dynamic light scattering correlation function; b) Powder X-ray diffraction pattern (simulated pattern above in gray); c, d) Scanning electron microscope images (scale bars = 500 nm, 5 μm, respectively).

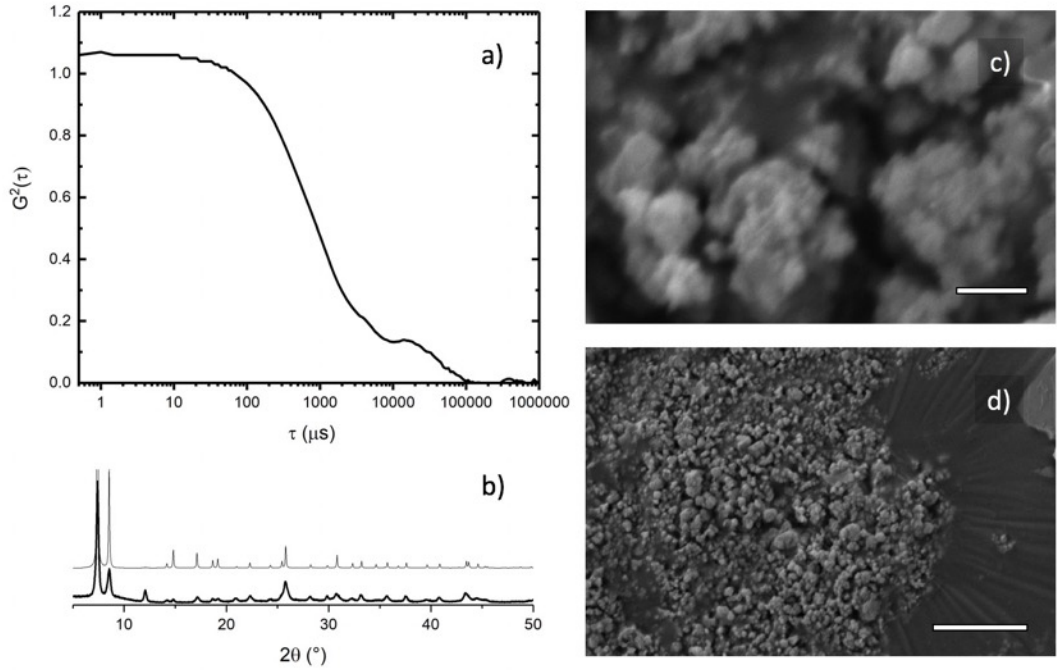

Figure S42. Characterization of UiO-66 modulated by 0.0003 equivalents of BA: a) Dynamic light scattering correlation function; b) Powder X-ray diffraction pattern (simulated pattern above in gray); c, d) Scanning electron microscope images (scale bars = 500 nm, 5 μm, respectively).

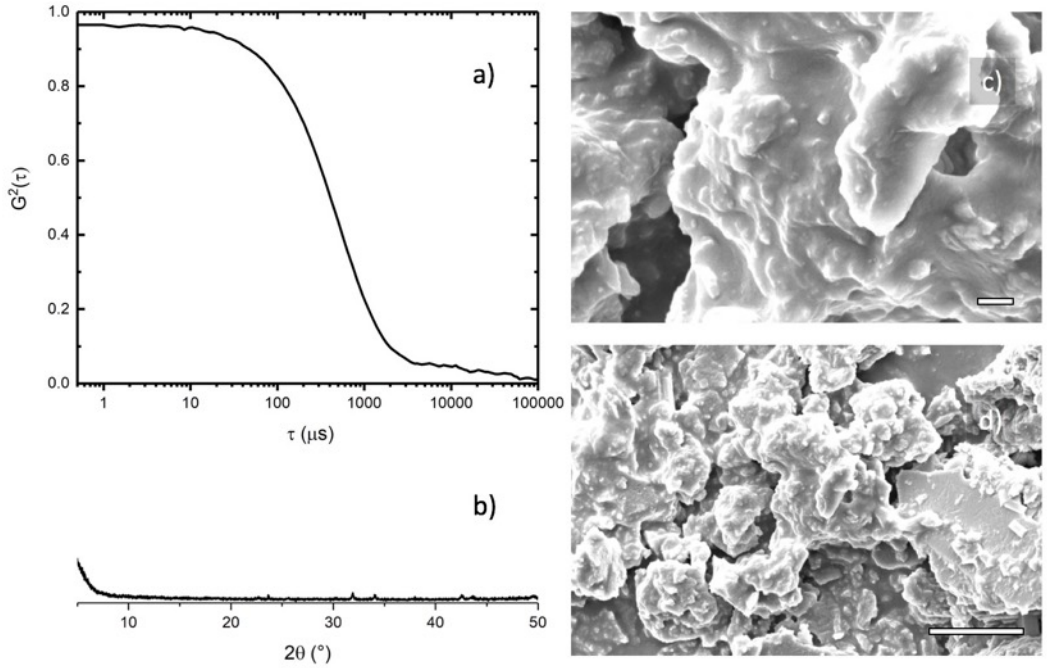

Figure S43. Characterization of UiO-66 modulated by 6 equivalents of PBA: a) Dynamic light scattering correlation function; b) Powder X-ray diffraction pattern (simulated pattern above in gray); c, d) Scanning electron microscope images (scale bars = 500 nm, 5 μm, respectively).

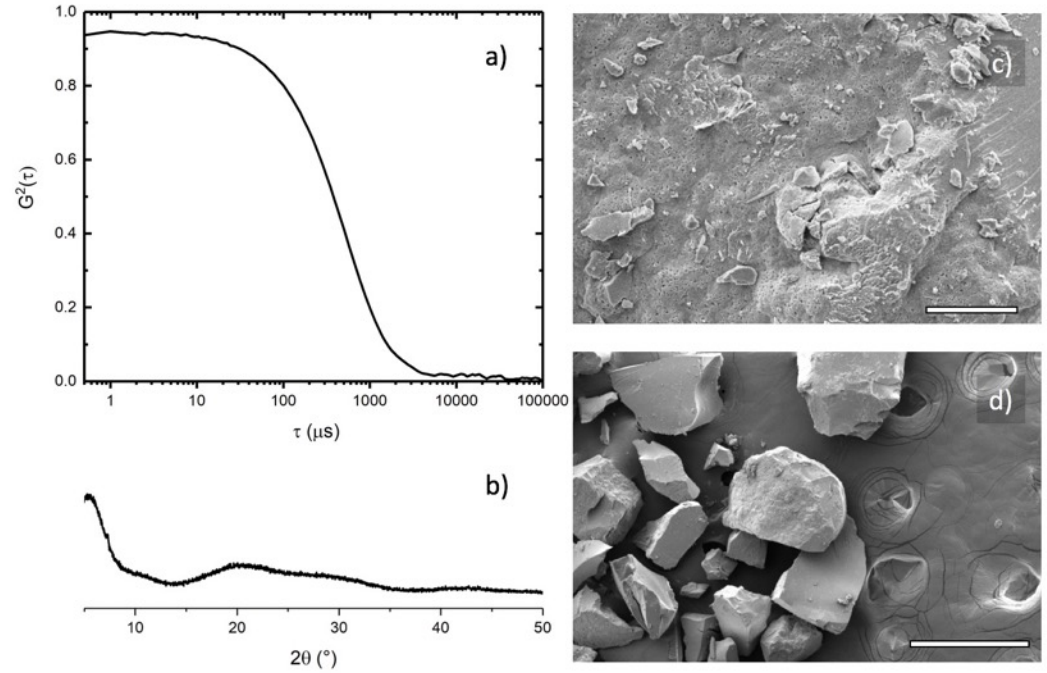

Figure S44. Characterization of UiO-66 modulated by 3 equivalents of PBA: a) Dynamic light scattering correlation function; b) Powder X-ray diffraction pattern (simulated pattern above in gray); c, d) Scanning electron microscope images (scale bars = 20 μm, 400 μm, respectively).

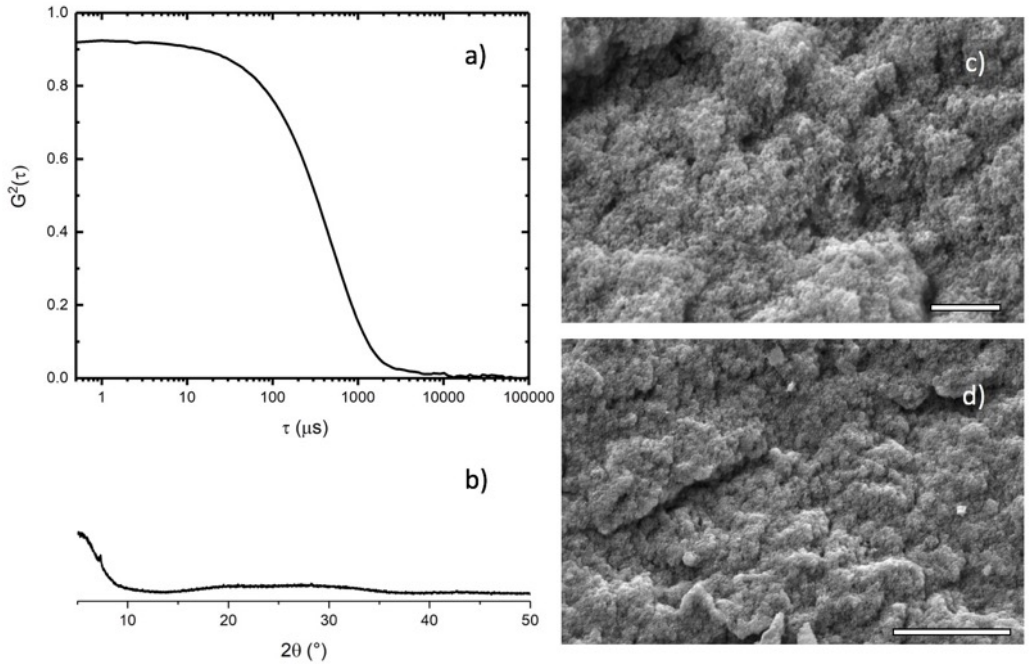

Figure S45. Characterization of UiO-66 modulated by 1 equivalent of PBA: a) Dynamic light scattering correlation function; b) Powder X-ray diffraction pattern (simulated pattern above in gray); c, d) Scanning electron microscope images (scale bars = 1 μm, 5 μm, respectively).

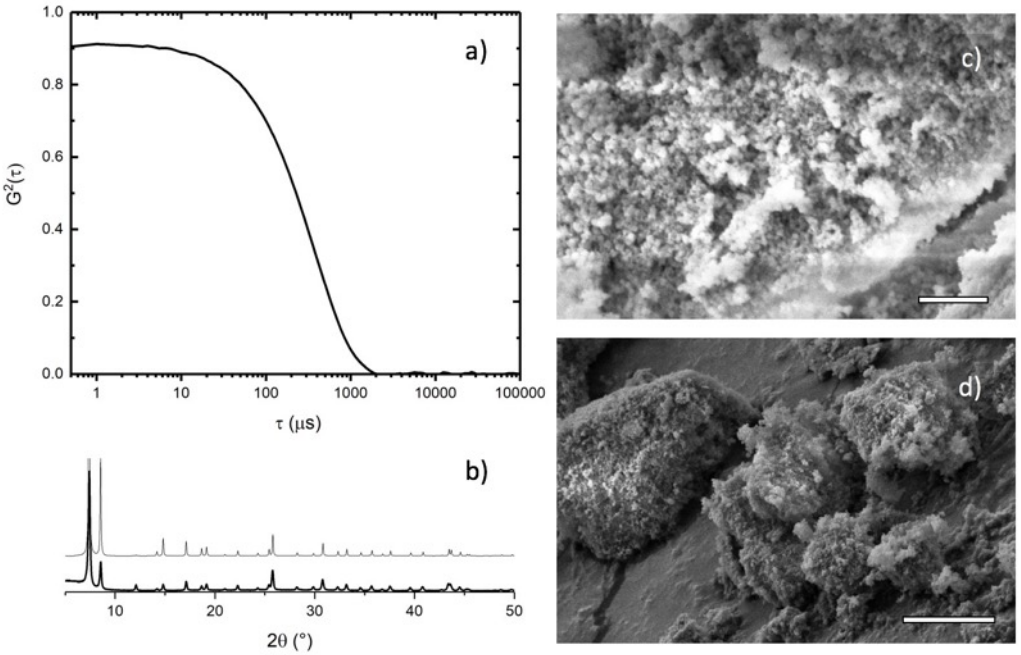

Figure S46. Characterization of UiO-66 modulated by 0.3 equivalents of PBA: a) Dynamic light scattering correlation function; b) Powder X-ray diffraction pattern (simulated pattern above in gray); c, d) Scanning electron microscope images (scale bars = 1 μm, 5 μm, respectively).

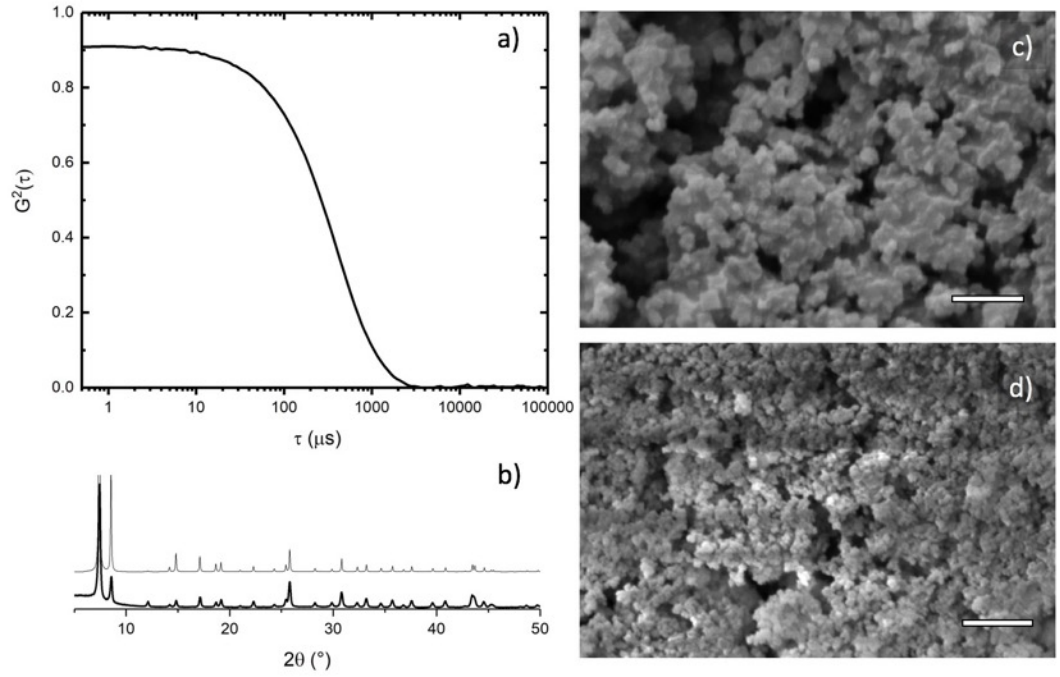

Figure S47. Characterization of UiO-66 modulated by 0.1 equivalents of PBA: a) Dynamic light scattering correlation function; b) Powder X-ray diffraction pattern (simulated pattern above in gray); c, d) Scanning electron microscope images (scale bars = 500 nm, 5 μm, respectively).

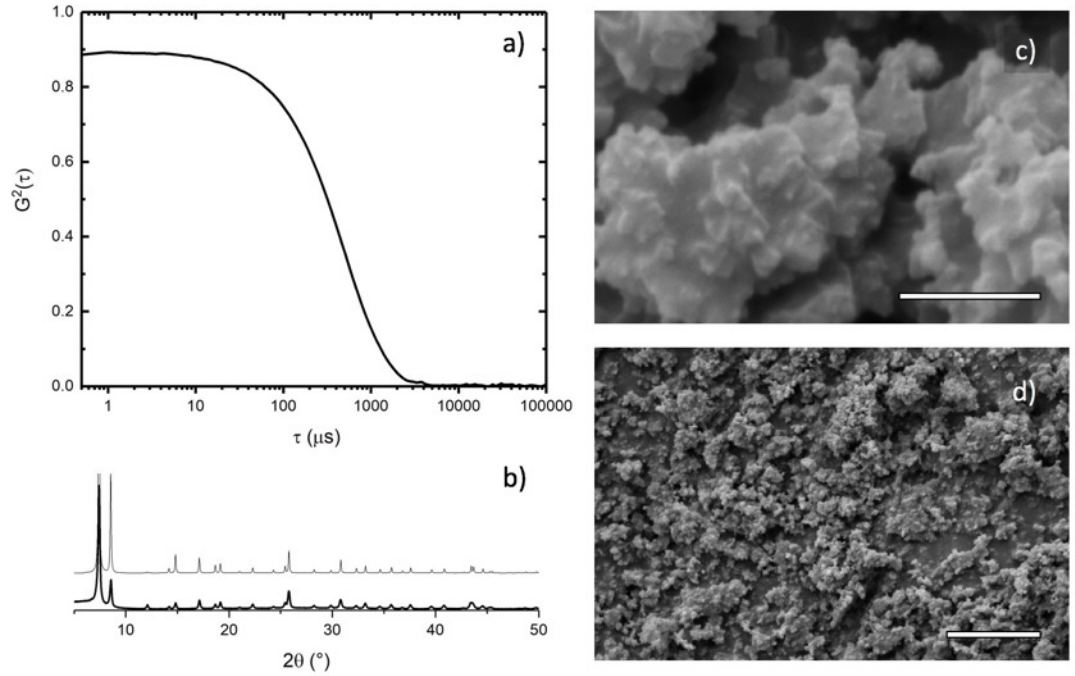

Figure S48. Characterization of UiO-66 modulated by 0.03 equivalents of PBA: a) Dynamic light scattering correlation function; b) Powder X-ray diffraction pattern (simulated pattern above in gray); c, d) Scanning electron microscope images (scale bars = 500 nm, 5 μm, respectively).

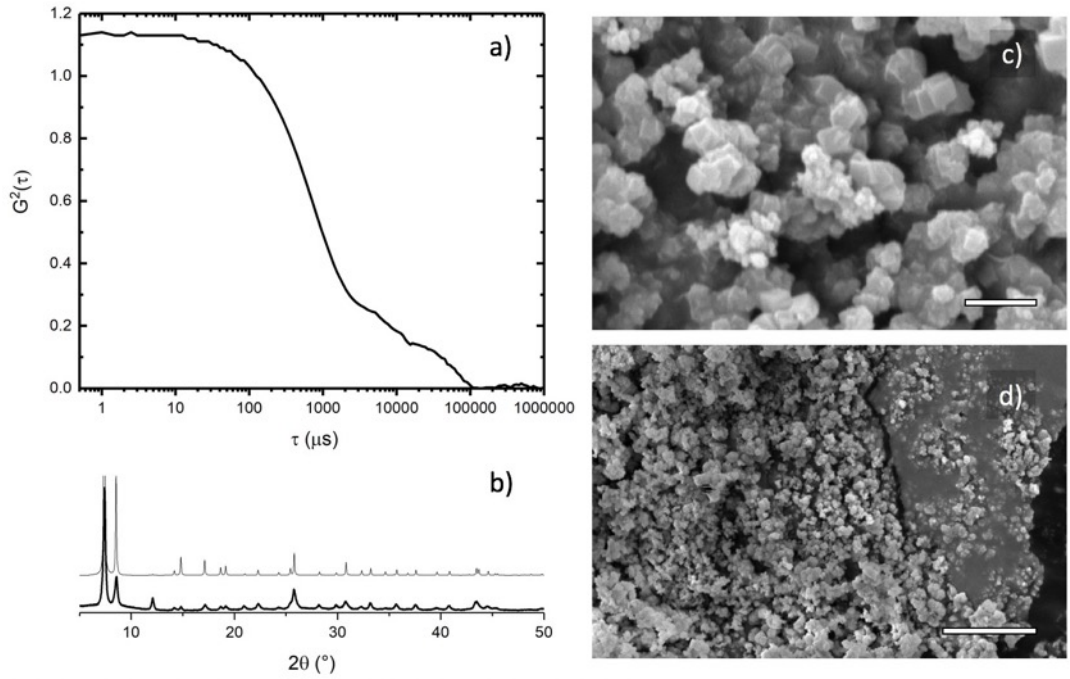

Figure S49. Characterization of UiO-66 modulated by 0.01 equivalents of PBA: a) Dynamic light scattering correlation function; b) Powder X-ray diffraction pattern (simulated pattern above in gray); c, d) Scanning electron microscope images (scale bars = 500 nm, 5 μm, respectively).

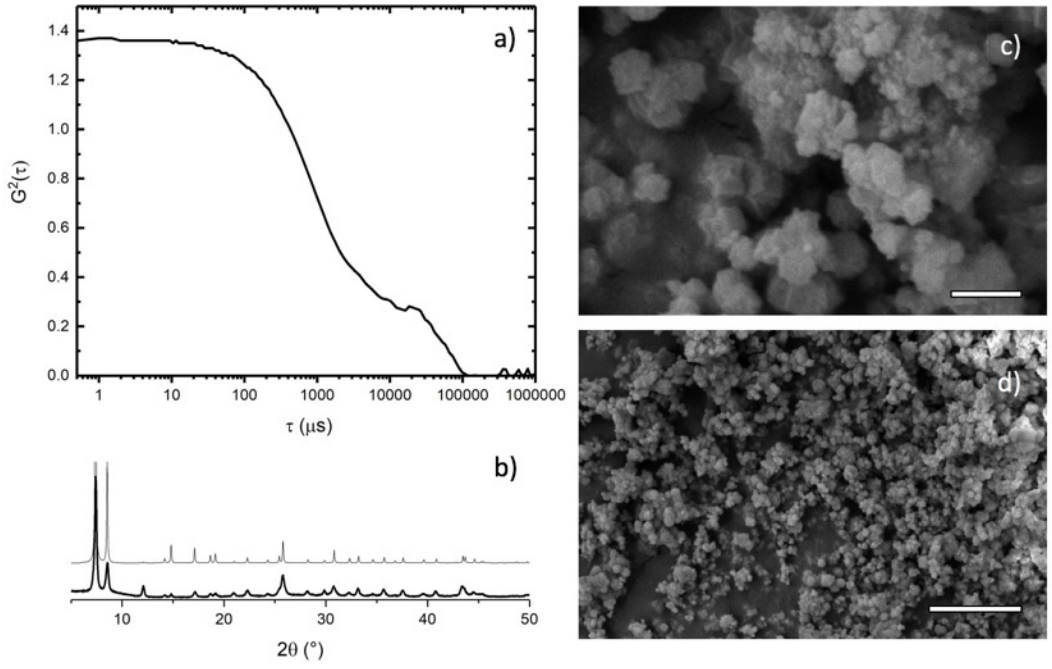

Figure S50. Characterization of UiO-66 modulated by 0.003 equivalents of PBA: a) Dynamic light scattering correlation function; b) Powder X-ray diffraction pattern (simulated pattern above in gray); c, d) Scanning electron microscope images (scale bars = 500 nm, 5 μm, respectively).

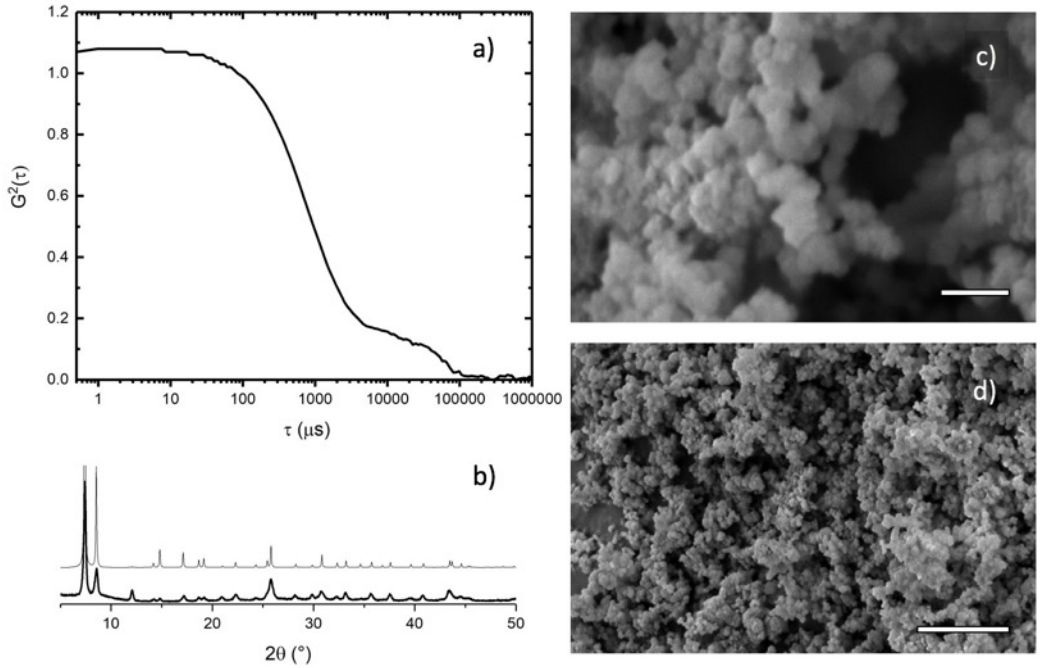

Figure S51. Characterization of UiO-66 modulated by 0.001 equivalents of PBA: a) Dynamic light scattering correlation function; b) Powder X-ray diffraction pattern (simulated pattern above in gray); c, d) Scanning electron microscope images (scale bars = 500 nm, 5 μm, respectively).

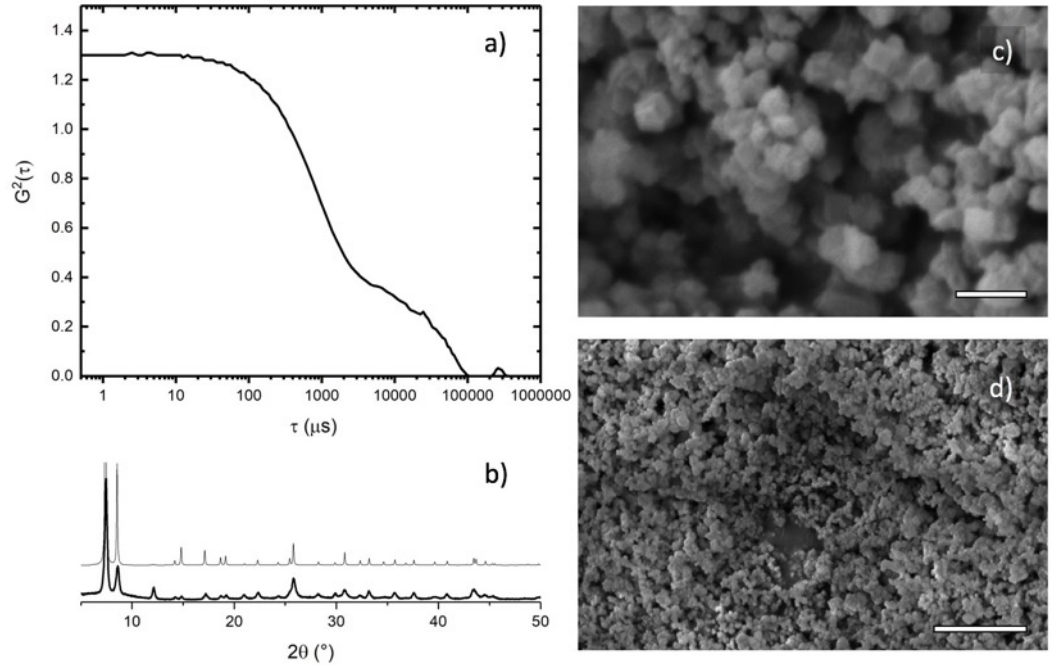

Figure S52. Characterization of UiO-66 modulated by 0.0003 equivalents of PBA: a) Dynamic light scattering correlation function; b) Powder X-ray diffraction pattern (simulated pattern above in gray); c, d) Scanning electron microscope images (scale bars = 500 nm, 5 μm, respectively).

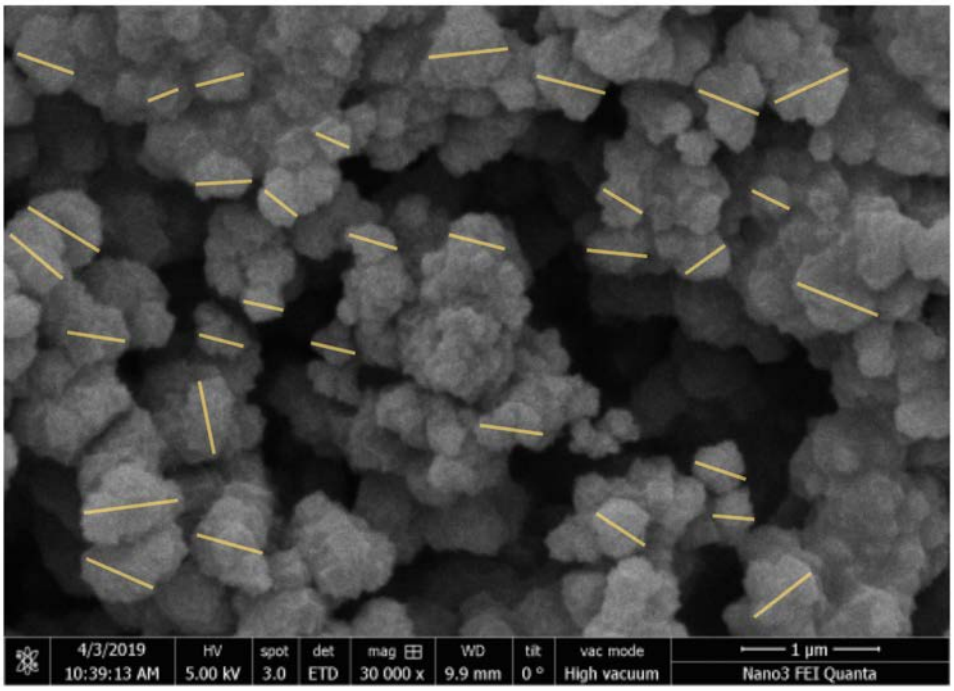

Figure S53. Determination of particle size for UiO-66 modulated by 0.03 equivalents of AA.

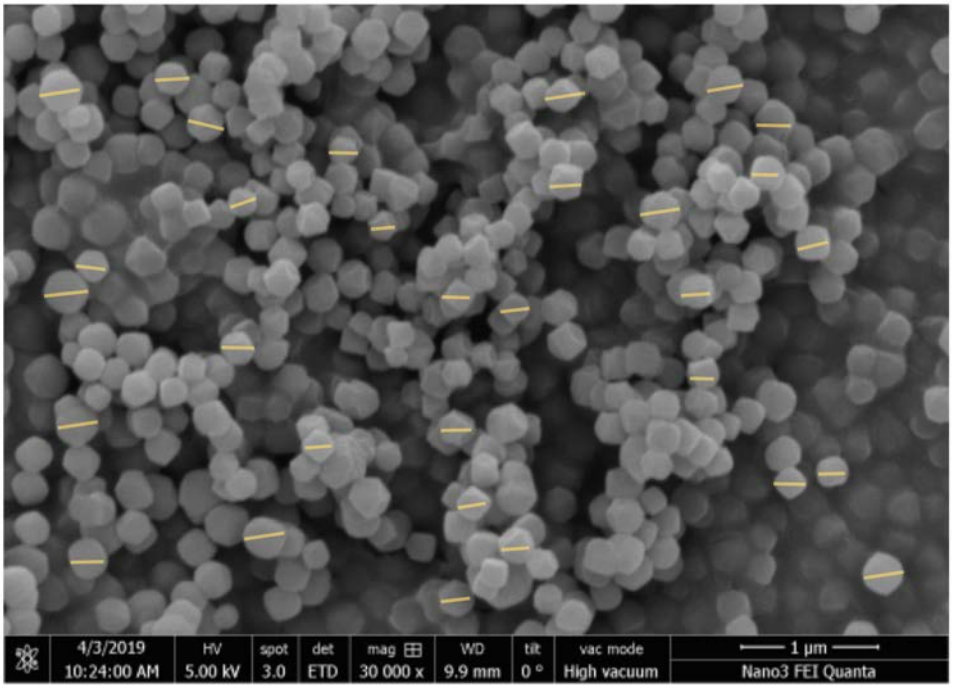

Figure S54. Determination of particle size for UiO-66 modulated by 30 equivalents of AA.

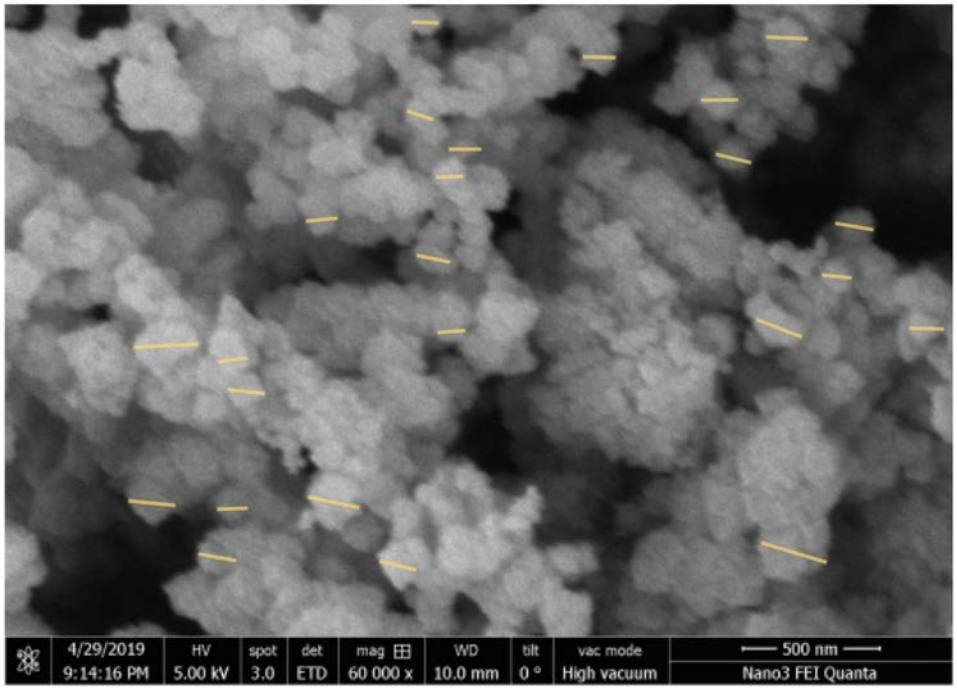

Figure S55. Determination of particle size for UiO-66 modulated by 0.0003 equivalents of PAA.

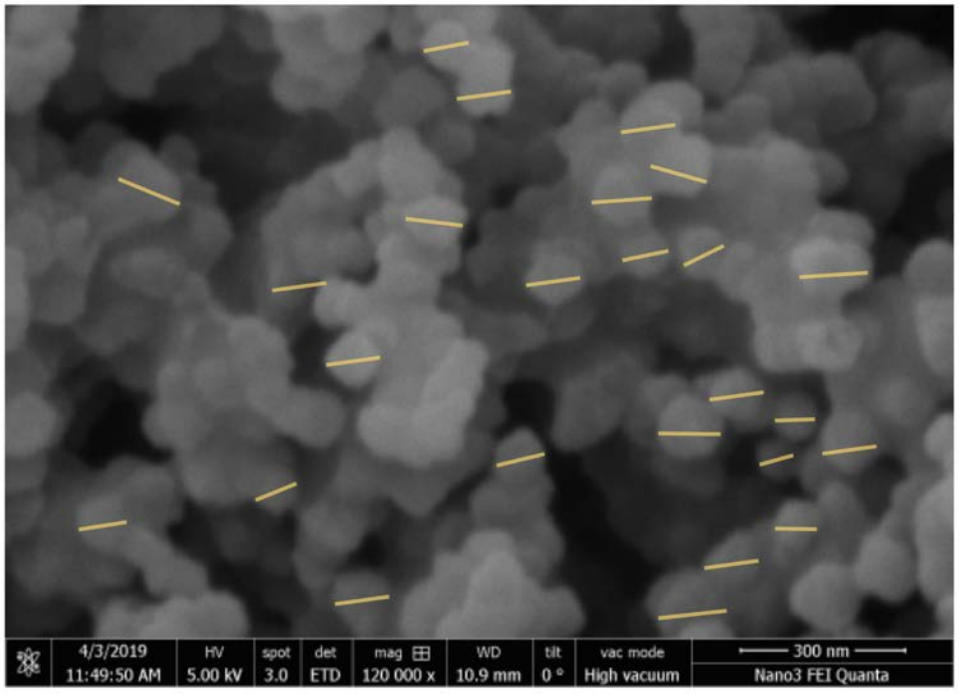

Figure S56. Determination of particle size for UiO-66 modulated by 3 equivalents of BA.

Table S1. BET surface areas from N_2 adsorption isotherms for select materials.

Modulator Type	Equivalents of acid	Surface area (m^2/g)
Acetic acid	30	1,229 ± 57
	1	716 ± 101
Poly(acrylic acid)	1	602 ± 52
	0.03	791 ± 41
Benzoic acid	10	1,046 ± 194
	0.3	1,018 ± 86
Poly(vinylbenzoic acid)	0.3	946 ± 13
	0.03	1,010 ± 25